Risk assessment of aristolochic acids in Indonesian jamu by predicting points of departure using the physiologically based kinetic modeling reverse dosimetry approach

10-03-2019

MSc thesis Toxicology

Charlotte Koopmans 930216464060

Toxicology Department

Wageningen University & Research

Stippeneng 4

6708 PB Wageningen

WAGENINGEN
UNIVERSITY & RESEARCH

Risk assessment of aristolochic acids in Indonesian jamu by predicting points of departure using the physiologically based kinetic modeling reverse dosimetry approach

10-03-2019

MSc thesis Toxicology

Charlotte Koopmans 930216464060

Supervisors

Suparmi

Dr. Sebas Wesseling

Prof. Dr. Ivonne M.C.M. Rietjens

WAGENINGEN
UNIVERSITY & RESEARCH

TABLE OF CONTENTS

LIST OF ABBREVIATIONS

AA	Aristolochic acid
AAN	Aristolochic acid nephropathy
BEN	Balkan endemic nephropathy
BMD	Benchmark Dose
$BMDL_{10}$	Benchmark Dose 10% Lower confidence limit
BMR	Benchmark Response
dA	Deoxyadenosine
dG	Deoxyguanosine
EDI	Estimated daily intake
FCS	Fetal calf serum
LC-MS/MS	Liquid Chromatography Mass Spectrometry/ -Mass Spectrometry
LoD	Limit of detection
LoQ	Limit of quantification
MOE	Margin of exposure
NADFC RI	National Agency for Drug and Food Control, Republic of Indonesia
PBK	Physiologically based kinetics
POD	Point of departure
RT	Room temperature
UPLC	Ultra performance liquid chromatography

ABSTRACT

Aristolochic acids (AAs) are toxic compounds, naturally occurring in *Aristolochia* and *Asarum* plants which are commonly used in traditional herbal medicines such as Indonesian jamu. AAs are known kidney carcinogens who need reductive activation to be able to form covalent DNA-adducts and eventually cause tumours. This reductive activation mainly occurs in the liver although the liver is not classified as the target organ of AA. In this present study, Indonesian jamu was analyzed for the presence of AAs via UPLC analysis and then the estimated daily intake (EDI) was calculated. Hereafter, an associated risk assessment based on liver toxicity was carried out using the margin of exposure (MOE) approach. Concentration-response curves for cytotoxicity and DNA-adduct formation were obtained by exposing human HepG2 and HepaRG cells to AA-I in vitro and with the physiologically based kinetic (PBK) modeling reverse dosimetry approach the obtained concentration-response curves were translated to predicted dose-response curves in vivo. Finally, the data from these predicted dose-response curves were used for BMD analysis to derive a $BMDL_{10}$ which was used for the risk assessment. Based on the UPLC analysis, two out of 15 samples (13.3%) appeared to contain AAs whereas the first sample contained both AA-I (21.6 µg/g) and AA-II (9.6 µg/g) and the second sample contained only AA-II (10.5 µg/g). The EDI was calculated to be 1.4 µg/kg bw for AA-I and 0.6 µg/kg bw for AA-II for the first sample and 1.0 µg/kg bw for AA-II for the second sample. Furthermore for the samples which were found to be negative for AAs, the LoD of 0.9 µM for AA-I and AA-II was used to calculate to possible EDI of AAs per sample. This EDI ranged in between 0.3 and 4.2 for AA-I and in between 0.1 and 1.1 for AA-II. The $BMDL_{10}$ as calculated for the liver cytotoxicity after translation to the in vivo dose-response situation was 2.66 mg/kg bw and was used for the risk assessment. MOE values were calculated for AA-I and AA-II individually and as combined exposure while assuming equal potency of cytotoxicity. For the liver cytotoxicity, All MOE values appeared to be above the threshold of 100. Based on the kidney cytotoxicity, all MOE values for AA-I and AA-II individually were above a 100. When taking into account the combined exposure, AA10 (99.5) and AA14 (93.4) had MOE values below 100 and thus indicating a priority for risk management. It is however questionable whether AAs in these samples are present since this was not detected by the UPLC analysis. Furthermore the MOE values based on the kidney cytotoxicity were a 5-fold lower as compared to the MOE values based on the liver cytotoxicity. From the present study it can be concluded that AAs are present in Indonesian jamu but that it is doubtful whether consuming Indonesian jamu regularly indicates a priority for risk management. Furthermore the present study confirms the current state of the art of the kidney being the target organ and not the liver, concluding that the kidney should stay the main focus for future research.

1. INTRODUCTION

1.1 BACKGROUND

1.1.1 ARISTOLOCHIC ACIDS, EPIDEMIOLOGY AND RISK OF EXPOSURE

Aristolochia and *Asarum* plants have been used for centuries in traditional herbal medicines and are known to contain Aristolochic acids (AAs). AAs are a group of nephrotoxic and carcinogenic compounds that occur mainly as 8methoxy-6-nitrophenanthro-(3,4-d)-1,3-dioxolo-5-carboxylic acid (AA-I) and its 8-demethoxylated form (AA-II) (Figure 1) (Heinrich et al., 2009; Kumar et al., 2003; NTP, 2016).

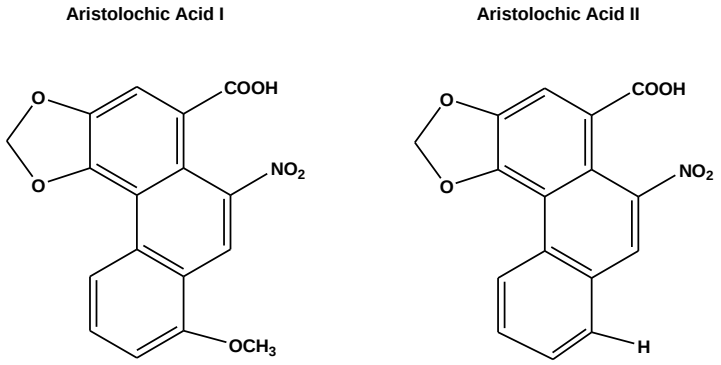

Figure 1: Molecular structure of AA-I and AA-II

The first AA poisoning was diagnosed in Belgium in 1991, where over 100 young women suffered from end-stage renal disease and in several cases cancer in the kidneys and the upper urinary tract. This incident was referred to as Chinese Herb Nephropathy, later renamed as Aristolochic Acid Nephropathy or AAN (Gillerot et al., 2001; L. J. Vanherweghem, 1998). The AA poisoning was due to the prolonged intake of a Chinese herb-based weight-loss preparation containing *Aristolochia fangchi* ('Guang Fang Ji') instead of *Stephania tetrandra* ('Han Fang Ji'). The mix-up of these two botanicals happened because the roots of the botanicals are both referred to as 'Fang Ji' in the Chinese lettering system 'Pin Yin' (Anderson & Vlietinck, 2000; IARC et al., 2002; L. J. Vanherweghem, 1998). Another possible mix-up in Pin Yin is 'Mu Tong', which used to describe *Aristolochia manshuriensis*, but also to describe certain *Clematis* or *Akebia* species such as *C. armandii*, *C. montana*, *A. quinata* and *A. trifolatia*. Furthermore, *Clematis* spp. such as *Clematis chinensis* Osbeck., may be adulterated with AA (FDA, 2001). Then, the Pin Yin name 'Mu Xiang', which describes *Aristolochia debilis* and other botanicals such as *Aucklandii lappa*, *Saussurea lappa* and certain *Inula* and *Vladimiria* species, doesn't give any evidence of substitution between the species, but the common names have potential for confusion in both the Chinese and Japanese language (Anderson & Vlietinck, 2000; IARC et al., 2002). Similar to incidences of AAN, in Balkan regions in the 1950's, AA exposure has been the causative agent responsible for the Balkan Endemic Nephropathy (BEN), a disease leading to chronic renal failure and urothelial cancer. BEN occurred after flour in the region was contaminated with *Aristolochia clematitis* and is considered as the environmental form of AAN (Arlt et al., 2002; Grollman et al., 2007; Hranjec et al., 2005; Jelaković et al., 2013).

After the incident in Belgium, more cases of AAN were reported in other countries including Spain, Japan, France, Belgium, UK, Taiwan, USA, Germany, China, Korea, Hong Kong, Australia and

Bangladesh (Jadot et al., 2017). Because of the severity of AAN and the past incidences, AAs got banned since 2001 in many countries worldwide (Debelle et al., 2008). Still, it appears that remedies containing AA have been and possibly are still being used in many regions in the world (Heinrich et al., 2009). In a study performed by Martena et al. (2007) was found that from the 190 Chinese herbal medicines that were analyzed between 2002 and 2006, 25 contained AA-I and 13 of these 25 also contained AA-II. Especially in the Asian area, AAN is potentially a crucial problem since a lot of people there still believe that traditional Chinese herb medicine are natural and thus safer than chemically produced 'Western' medicine (Hong et al., 2006). In contrast, risk assessment of AA exposure shows that the use of certain Chinese herbal medicine significantly increases the risk of upper tract urothelial carcinoma and that there is a dose-dependent relationship between cumulative AA exposure and the risk of developing end-stage renal disease (F. Wu & Wang, 2013).

1.1.2 INDONESIAN JAMU

Indonesian jamu is one of the traditional herbal medicines that has been used for many centuries in the Indonesian community to maintain good health and to treat all kinds of diseases (Elfahmi et al., 2014). Indonesian jamu is usually made of different parts of plants such as leaves, bark, roots and flowers that are characteristically mixed together to get the desired herbal preparation (Afdhal & Welsch, 1988). Since the 1980's, small Indonesian jamu producers started to grow strongly which led to Indonesian jamu production on a larger scale and in a range of formulations like powders, pills, capsules, crude extracts, tablets and liquids (Beers, 2012; Woerdenbag & Kayser, 2014). Nowadays, an estimated 49.0% out of 294962 Indonesian households consumes Indonesian jamu preparations as a medicine. The reasons for use are: health and physical fitness (52.7%), more efficacious (18.4%), as a tradition and the believe that natural is good for health (12.3%), low cost (6.8%), trial and error (2.8%) and as an option when medicinal treatment did not work (1.8%) (MoH, 2013). However, the efficacy is still largely based on experience and empirical facts and thus more research is needed to scientifically prove efficacy and to assure safety of Indonesian jamu (MoH, 2007).

In the last decade it became clear that 'natural' does not equal 'safe', and that botanicals and herbal preparations might contain compounds that are toxic to humans (Rietjens et al., 2005). The current Indonesian law has not explicitly regulated the maximum limit of natural compounds present in Indonesian jamu. Moreover, The National Agency for Drug and Food Control, Republic of Indonesia (NADFC RI) published several reports related to the adverse health effects of the consumption of herbal medicines and health supplements, 48 in 2015 and 16 in 2016 respectively (NADFC, 2015, 2017). One of these reports showed that the carcinogenic compounds aflatoxin B1, B2 and G2, toxins produced by diverse *Aspergillus* species, were present in 11 Indonesian jamu samples (Ali et al., 2005). In 2018, 25 samples of Indonesian jamu have been evaluated for the presence of alkenylbenzenes, a group of compounds that are genotoxic and carcinogenic, such as estragole, methyleugenol, elemicin, safrole, myristicin and apiol. The study found that 23 out of 25 Indonesian jamu samples contained alkenylbenzenes and that 20 out of 25 samples raised a health concern for humans when consuming the Indonesian jamu regularly (Suparmi et al., 2018). Furthermore, a risk assessment has been performed previously for AAs in herbal supplements. In this study was found that 3 out of 18 samples contained AAs and that those samples were a priority for risk management based on tumour formation

(Abdullah, 2017). Because of the findings of these recent studies and the knowledge that *Aristolochia* and *Asarum* plants are widely used in traditional herbal medicines, it is of importance to evaluate Indonesian jamu for the presence of aristolochic acids and see if they pose a health concern.

1.1.3 Metabolic pathways, cytotoxicity and DNA-adduct formation upon exposure of AAs

AAs have been classified by IARC in group 1, which means that there is sufficient evidence that they act as carcinogens in humans (IARC, 2012). Both AA-I and AA-II are compounds that are mutagenic and genotoxic after reductive activation in vitro and in vivo. After this activation they can form covalent DNA adducts and these are considered as one of the primary steps of the development of cancer (Guengerich, 2000; Mei et al., 2006; Joelle L Nortier et al., 2000). In this study, the focus for DNA-adduct formation will be on AA-I since this is the most abundant one (Tian-Shung et al., 2005).

There are two metabolic pathways, the detoxification pathway and the reductive activation pathway, that influence the ability of AAs to cause adverse effects in the human body. The detoxification pathway decreases the amount of AAs that can cause harm in the body by metabolizing the AAs to their less toxic metabolites which are excreted by the feces and urine (M Stiborová et al., 2008). So far, the only detoxification metabolites that are found to be excreted by humans are aristolactam I and II (EMEA, 1997). The major activation pathway of AA involves nitroreduction to an electrophilic cyclic *N*-acylnitrenium ion with a delocalized positive charge. These ions can bind to the exocyclic amino groups of purine bases, forming covalent DNA-adducts (Figure 2) (Pfau et al., 1990; Stiborová et al., 2017). To induce this nitroreduction, NAD(P)H:Quinone Oxidoreductase (NQO1) is the most important enzyme in human, mouse and rat for activating AA-I in hepatic and renal cytosolic subcellular fraction (Arlt et al., 2002; M. Chen et al., 2011; Martinek et al., 2011). Also hepatic microsomal cytochrome P450 (CYP) 1A1/2 and kidney microsomal NADHP:CYP reductase (POR) have shown that they are able to allow reduction of AA-I (Milichovský et al., 2016).

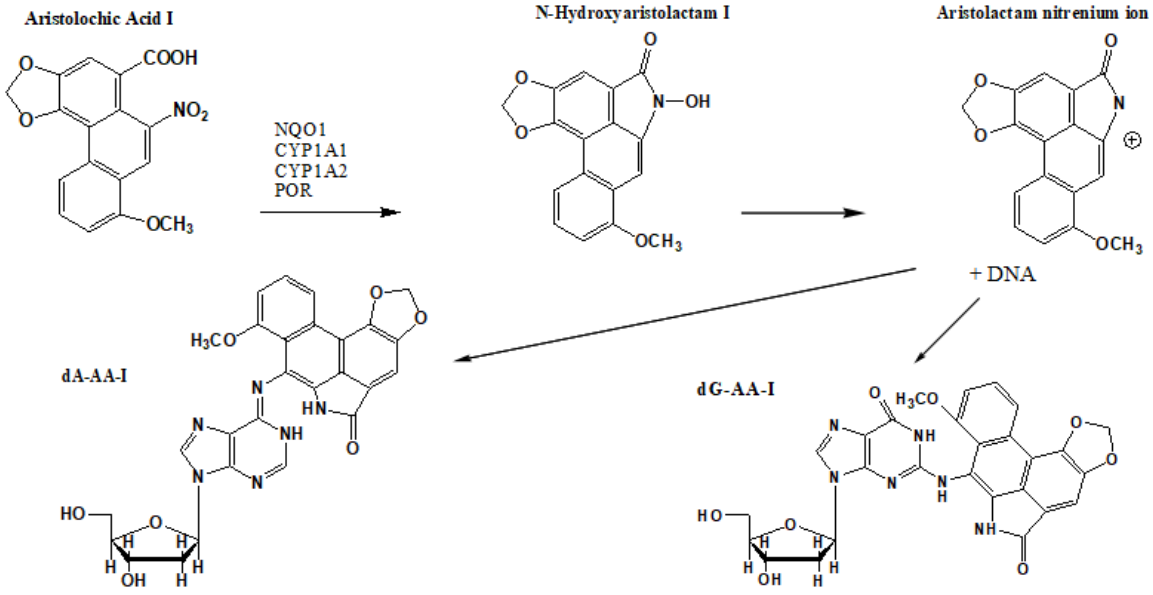

Figure 2: Reductive activation of AA-I and the formation of DNA-adducts

In humans, the predominant DNA-adducts of AA-I are 7-(deoxyadenosin-***N***^{6}-yl) aristolactam I (dA-AA-I) and 7-(deoxyguanosin-***N***^{2}-yl) aristolactam I (dG-AA-I) where dA-AA-I has found to be the most persistent, leading to an excess of AAG to TAG (A: T → T: A) transversions. The highest fraction of these transversion mutations occur in the kidney and the bladder (Grollman et al., 2007; Pfau et al., 1990; Rosenquist & Grollman, 2016). In AAN patients, an overexpression of protein p53 was observed suggesting a mutation in the tumour suppressor gene of p53 (Cosyns et al., 1994). This mutation was later identified as the specific AAG to TAG transversion mutation in codon 139 (Lys → Stop) of exon 5 in the p53 gene and is now recognized as the mutational signature and used as another indicator for AA exposure (Lord et al., 2004; Rosenquist & Grollman, 2016).

As already stated before, AAs are proven to be nephrotoxic and the upper urinary tract and kidneys are the target organs. The liver is however classified as a non-target organ, even though reductive activation takes place in both the liver and the kidneys (Mei et al., 2006). The reason for the difference in effect of AA-I exposure in the organs remains unclear. In a study performed by L. Zhang et al. (2007), a 5-fold higher cytotoxicity in the human hepatic Bel-7402 cells was found as compared to the human kidney HK-2 cells upon an exposure level of 82.2 µM AA-I (IC_{50}), which is controversial to the expectations. This IC_{50} was comparable to the IC_{50} of 70.3 µM AA-I for cytotoxicity found in the human hepatic HL-7702 cells by Liu et al. (2015) and the development was in a concentration-dependent manner. Moreover, an IC_{50} in the human fetal hepatic L-02 and IC_{75} in the human hepatoma HepG2 cells were observed after an exposure level of 58.6 µM AA-I as reported by Yuan et al. (2009) and Nitzsche et al. (2013) respectively. Both of these assays also showed the cytotoxicity in a concentration-dependent manner. Even higher cytotoxic effects were observed in HepG2 cells when exposed to the mother tincture of *A. clematitis* or *A. europaeum* although this might be due to unknown compounds present in the tincture (Nitzsche et al., 2013). Furthermore, previous studies have shown significantly increasing numbers of micronuclei in HepG2 cells after AA exposure (Kevekordes et al., 2001; K. Wu et al., 2007).

As for the DNA-adduct formation, in a Belgian AAN patient who took the weight loss preparations mentioned earlier for 14 months, significant levels of dA-AA-I were detected post-mortem in the tissues from not only the kidney but also the liver, pancreas, lymph nodes, stomach and lungs (Joëlle L Nortier et al., 2003). Then, a French AAN patient who took a herbal preparation containing AA for 12 months showed similar amounts of dA-AA-I between the urinary tract and the liver and a way lower amount of dA-AA-I in the kidney. In addition, necrotic tissue and a carcinoma with a transitional cell origin was observed in the liver (Arlt et al., 2004). Furthermore, Lord et al. (2004) found that in a patient who was diagnosed with AAN and later got a breast carcinoma that metastasized to the liver, dA-AA-I was found all three organs.

Based on the results of previous studies on the cytotoxicity of AA-I on hepatic cell lines, the results of the formation of dA-AA-I in the liver of the described AAN patients and taking into account the metabolic activation of AA-I in the human liver, there are strong reasons to assume that upon AA-I exposure problems will not only occur in the kidney and the upper urinary tract but also in the liver. Therefore, the effects of AA-I exposure upon the human liver need to be studied more extensively.

1.1.4 MARGIN OF EXPOSURE

The risk assessment of AAs in Indonesian jamu should be carried out to determine whether risk management actions are needed to protect human health. For carcinogenic compounds, the previous advice was to use the as low as reasonably achievable (ALARA) approach to protect human health. However, this advice didn't take into account either the exposure level nor carcinogenic potency. JECFA then concluded that from the alternative approaches, the margin of exposure (MOE) approach was the recommended option. This harmonized MOE approach is now recommended by the European Food Safety Authority (EFSA), the Joint FAO/WHO Expert Committee on Food Additives (JECFA) and the International Life Sciences Institute (ILSI) (Barlow et al., 2006; Benford et al., 2010; EFSA, 2005; FAO/WHO, 2005). Previous use of the MOE approach already showed the risk of genotoxic and carcinogenic compounds in plant food supplements and other herbal products (Abdullah, 2017; Van Den Berg et al., 2011). Using the $BMDL_{10}$, which is the lower confidence limit of the benchmark dose giving 10% extra incidence, is considered the most appropriate point of departure (POD) for calculating the MOE, since it accommodates uncertainty in the data, taking into account a factor 10 for interspecies and a factor 10 for intraspecies. The outcome of the MOE below 10 000 is considered a priority for risk management based on carcinogenicity data and a lifetime exposure. When using non-carcinogenic data to do risk assessment, a MOE below 100 is considered a priority for risk management (Barlow et al., 2006; Benford et al., 2010; EFSA, 2005; FAO/WHO, 2005).

1.1.5 PHYSIOLOGICALLY BASED KINETIC MODELING REVERSE DOSIMETRY APPROACH

To carry out the MOE approach, the $BMDL_{10}$ can be derived from available in vivo tumour data. In case of lack of in vivo data, the $BMDL_{10}$ can be predicted by using the physiologically based kinetic (PBK) modeling approach. PBK models are used to describe the time-dependent absorption, distribution, metabolism and excretion of a certain amount of a substance in a living system which enables the translation of in vitro concentration-response data to in vivo dose-response data (Gerlowski & Jain, 1983). PBK modeling has previously adequately predicted PODs for acute liver toxicity by pyrrolizidine alkaloids (L. Chen et al., 2018), uterus growth caused by estrogenic chemicals (M. Zhang et al., 2018), developmental toxicity by glycol ethers (Louisse et al., 2010) and toxicity and DNA-adduct formation in the kidney by AAs (Abdullah, 2017). The steps for PBK modeling were followed as described by Abdullah (2017) which are similar to the methods of the other studies.

The first step is important to decide on an in vitro model which could be used to obtain concentration-response curves for the compound of concern. HepG2 cells have been used often in in vitro AA exposure assays (Kevekordes et al., 2001; Nitzsche et al., 2013; K. Wu et al., 2007) and it is well documented that HepG2 cells retain the activity of several phase I enzymes involved in reductive activation such as cytochrome P450 CYP1A1/2 as well as several phase II enzymes and it reflects the metabolism in vivo better than experimental models with metabolically incompetent cells and exogenous activation mixtures (Knasmüller et al., 1998). HepaRG cells have been reported previously to be a useful hepatic cellular model for in vitro toxicity studies based on their high drug metabolizing enzyme activities and stable expression of liver-specific functions (Jennen et al., 2010; Kanebratt & Andersson, 2008; Yokoyama et al., 2018).

The second step implies the development of the PBK model. In this step decisions on which organs were relevant for the PBK model to give a separate compartment and which organs could be put together as either slowly perfused tissue (e.g. bones, skin) or rapidly perfused tissue (e.g. heart, brain) are made. Each compartment will have their own physiological parameters which were blood flows to tissue and tissue volumes, physicochemical parameters which were the partition coefficients and kinetic parameters which were biotransformation reactions relevant for the chemical (Clewell & Clewell III, 2008; Krewski et al., 1994; Krishnan & Andersen, 2001; Rietjens et al., 2011).

The third step involves evaluation of the model by comparing the predicted concentration values by in vivo kinetic data available from the literature. When validated, the PBK model can be used to translate the in vitro concentration-response curves to in vivo dose-response curves.

Step four consists of the translation to in vivo dose-response curves via the reverse dosimetry approach. All concentration levels used in the in vitro models should be set to the maximum concentration (C_{max}) in the relevant tissue so it can be determined which predicted oral dose belongs to the C_{max}.

The fifth step is the BMD analysis to derive a $BMDL_{10}$ as POD for risk assessment using the predicted in vivo dose-response curve from the previous step.

The final step is doing the evaluation of the predicted $BMDL_{10}$ by comparing this $BMDL_{10}$ to in vivo derived $BMDL_{10}$ values as obtained by the literature.

1.2 AIM OF THE STUDY

The aim of the present study was to determine the presence and levels of AAs in Indonesian jamu and to perform an associated risk assessment to see whether there is a priority for risk management. The Indonesian jamu samples were analyzed by UPLC analysis to determine the levels of AA-I and AA-II in the samples. To derive a POD for risk assessment, In vitro cytotoxicity and DNA-adduct formation assays were performed using HepG2 and HepaRG cells as in vitro models to obtain concentration-response curves. These concentration-response curves were then translated to in vivo dose-response curves by applying the PBK modeling reverse dosimetry approach. Hereafter, the translated dose-response data was used for BMD analysis to derive a $BMDL_{10}$. With this $BMDL_{10}$, the risk assessment for human liver cytotoxicity was carried using the MOE approach. Finally, the outcomes of the risk assessment for the liver cytotoxicity were put into perspective by also performing the risk assessment for human kidney cytotoxicity based on available $BMDL_{10}$ values.

2. MATERIALS AND METHODS

2.1 ANALYSIS ON THE PRESENCE OF ARISTOLOCHIC ACIDS IN INDONESIAN JAMU

2.1.1 COLLECTED SAMPLES

In total, 15 Indonesian jamu samples were collected from Indonesia (Table 1). When collecting the samples, the focus was set on the Indonesian jamu that contained the botanicals *Aristolochia* or *Asarum*. Also, botanicals that had similar Chinese Pin Yin names as *Aristolochia* or *Asarum* or botanicals which may be adulterated with AA were taken into account. In this case, the selected botanicals were *Aristolochia debile* Sieb.Et.Zucc., *Herba Asari* (*Asarum sieboldii* Miq.), *Stephania tetrandra* S. Moore, *Clematis armandii*, *Clematis chinensis* Osbeck*., Aucklandii lappa* and *Saussurea lappa* and are stated in bold in Table 1. The name of the plant species in the ingredient list of the Indonesian jamu was used as stated of the package or searched for on KNApSAcK Family in the 'jamu' section by Afendi et al. (2011).

Table 1: Characteristics of Indonesian jamu samples

Sample ID	Name	Ingredients: plant species	Form and content per unit	Recommended daily intake	preparation method	Health claims
AA1	Sendi	*Zingiberis officinale* Rosc. extract (1.75 g), *Curcumae domestica* Val extract (1.4 g), *Curcumae aeruginosa* Roxb. (1.05 g), *Languatis* rhizoma extract (910 mg), *Myristicae* semen (700 mg), ***Saussurea lappa*** (700 mg), *Zingiberis officinale* Rosc (350 mg), *Retrofracti* Fructus (140 mg)	Sachet 7 g	1-2 times a day	Mix a sachet of SENDI into a half glass of hot water (100cc), add a few drops of lemon juice and honey.	For stiffness, muscle and joint pains. Help to refresh and warm the body.
AA2	Arum Bulan	*Curcumae domestica* Val (1 g), *Parameriae* Cortex (750 mg), *Andropogon zizanoides* (500 mg), *Arecae* Semen (500 mg), other ingredients up to (5 g) e.g. ***Saussurea lappa***	Sachet 5 g	1 time a day	one sachet, brewed with 100 ml warm boiled water	Helps reduce excessive mucus, vaginal discharge and odor less pleasant for women. Helps to nourish to body for a woman who was menstruating.
AA3	Sabdo Lancar Haid	*Curcumae xanthorrhiza* Roxb (500 mg), *Languas galanga* Stunz (500 mg), *Alyxiae reinwardtii* Bl. (250 mg), *Piper nigrium* L. (250 mg), other ingredients up to (5 g) e.g. ***Saussurea lappa***	Sachet 5 g	1 time a day	one sachet, brewed with 100 ml warm boiled water	Helps expedite and ease the aches and pains during menstruation
AA4	Renkap (Hua Tao Sie Lin)	*Acanthopanax senticosus* (800 mg), ***Clematis chinensis* Osbeck.** (600 mg), *Notopterygium insicum* (600 mg), *Angelica pubescentis* (600 mg), *Achryranthes bidentata* Blume (600 mg), ***Stephania tetrandra* S. Moore** (400 mg), *Carthamus tinctorius* L. (400 mg)	Capsule 400 mg	2 x 2 times a day		Helps to decrease stiffness, gout and muscle pain
AA5	Regalin (Feng Thong Pao)	*Acanthopanax senticosus* (15%), ***Clematis chinensis* Osbeck.** (15%), *Lycium barbarum* L (10%), Charthamus *tinctorius* L. (10%), ***Herba Asari (Asarum sieboldii* Miq.)** (10%), *Notopterygium incisum* (10%), *Schisandra chinensis* (Turcz.) Baill. (10%), *Gardenia augusta* Merr. (10%), *Angelica dahurica* (5%), *Saposhinkovia divaricata* (Turcz.) Schischk. (5%)	Capsule 500 mg	2 x 3 times a day	Before/ after a meal, drink with warm water	help treat and prevent gout, stiffness, joint muscle aches and prevent rheumatic symptoms

AA6	Ginggaroo (Teng Chuan Hoa Tam Wan)	*Panax ginseng* L.(22.5 mg), *Fritillaria cirrhosa* D. Don (33.75 mg), *Aquilaria sinensis* (15 mg), *Astragalus membranaceus* (Fisch. ex Link) Bunge (22.5 mg), *Atractylodis* Macrocephala (18,75 mg), Schizandiae Fructus (18,75 mg), Platycodi Fructus (18.75 mg), ***Aristolochia debile* Sieb.Et.Zucc.**	Pill 150 mg	8 x 3 times a day		To help pacify cough with phlegm
AA7	Delitik (Thien Ma Ren Sen Su Lok Yen)	*Panax ginseng* L. extract (25 mg), *Gastrodia elata* Bl. extract (75 mg), *Psoraleae coryfolia* L. extract (25 mg), *Atractylodis* Rhizoma extract (50 mg), *Glycyrrhizae glabra* L. extract (25 mg), ***Clematis chinensis* Osbeck. extract** (25 mg), *Evodiae rutaecapra* (Juss.) Benth. extract (25 mg)	Capsule 250 mg	3-4 x 3 times a day	Drink with warm water	Traditionally used to help treat sore rheumatic pain
AA8	Sendi	*Zingiberis officinale* Rosc extract (165 mg), *Curcumae domesticae* Val extract (110 mg), *Curcumae aeruginosae* rhizoma extract (82.5 mg), *Languatis* rhizoma extract (71.5 mg), *Myristicae* semen extract (55 mg), ***Saussurea lappa*** radix extract (55 mg), *Retrofracti* fructus extract (11 mg)	Capsule 550 mg	2 x 2 times a day		For stiffness, muscle and joint pains
AA9	Antra Kapsul (Pien Tze Wuang Yen Tu Jing)	*Coptis chinensis* Franch. (750 mg), *Plantago major* L. (750 mg), *Taraxacum officinale* Wiggers (750 mg), *Andrographis paniculata* Ness (750 mg), ***Asarum sieboldii* Miq.** (500 mg), *Arctium lappa* L. (500 mg), Phellodendron *chinense* Schneid. (500 mg), *Nothopanax scutellarium* Merr. (500 mg)	Capsule 500 mg	2 x 3 times a day		Helps to cure fever and to reduce swelling
AA10	Anturin (Neo Shi Lin)	*Clerodendranthus spicatus* (16%), ***Herba asari (Asarum sieboldii* Miq.)** (15%), *Lysimacia christinae* Hance (20%), rhizoma *Imperatae* (15%), *Medulla junci* (24%), Glycyyrriza *glabra* L. (10%)	Pill 300 mg	5 x 3 times a day		Promotes a healthy urinary tract and prevent symptoms of urinary tract infections
AA11	Beuric (Niau Xuan Wan)	*Panax ginseng* L. (500 mg), *Salvia miltiorrhiza* Bge. (500 mg), *Cistanches salsa* (500 mg), *Polygonum multiflorum* rhizoma (400 mg), *Drynaria sparsisora* Moore (400 mg), *Cibotium barometz* J. Sm. (400 mg), *Eucommia ulmoides* (500 mg), *Rehmannia preparata* (400mg), *Spatholobus suberectus* Dunn (400 mg), *Epimedium brevicornum* Maxim (400 mg), ***Clematis chinensis* Osbeck.** (250 mg), *Uncarcia rhynchophylla* (Miq.) Jacks. (400mg)	Capsule 500 mg	2 x 3 times a day	Drink with warm water	helps maintain healthy kidney function and traditionally helps blood circulation

AA12	Liparkap	*Bubleurum falcatum* (200mg), *Lysimachia christinae* Hance (200 mg), *Artemisia scopariae* Waldst. et Kit. (200 mg), ***Clematis armandii*** **Franch.** (160 mg), *Rehmannia preparata* (180 mG), *Plantago major* L (180 mg), *Paeonia lactiflora* pall. (140 mg), *Saposhinkovia divaricata* (Turcz.) Schischk. (140 mg), *Citrus aurantium* (120 mg), *Coptis chinensis* Franch. (120 mg), *Nothopanax scutellarium* Merr. (120 mg), *Gardenia augusta* Merr. (120 mg)	Capsule 500 mg	2 x 3 times a day		Helps to cure fever and helps maintain healthy liver functioning
AA13	Andis	*Rheum officinale* Baill(16 mg), *Areca catechu* L (24 mg) , *Acorus calamus* L. (16 mg), *Carum copticum* Benth (4 mg), ***Saussurea lappa*** (4 mg), *Magnolia officinalis* Rehd. (16 mg), *Nothopanax scutellarium* Merr. (16 mg), *Atracty0loidis* Macrocephala (16 mg), *Piper retrofractum* Vahl. (16 mg), *Amomum cardamomum* Willd (16 mg), *Paeonia lactiflora* pall. (16 mg), *Mentha piperita* L (0.004 mg), *Eucalyptus alba* Reinw (0.008 mg), Etanolum ad (5 mg)	Liquid 5 ml	1 x 1 bottle	Mix the bottle with 1/2-1 cup of boiled water	For stomach ache
AA14	Sehat Lambung (Xiang Sha Yang Wei Wan)	***Aucklandii lappa*** (16mg), *Amomum kravanh* Pirre ex Gagnep (16 mg), *Atractylodis* Macrocephala (22 mg), *Citrus reticulata* Blanco (22 mg), *Wolfiporia extensa* (Peck) Ginns (22 mg), *Cyperus rotundus* L (16 mg), *Citrus aurantium* (16 mg), *Amomum kravanh* Pirre ex Gagnep (16 mg), *Magnolia officinalis* Rehd. (16 mg), *Pogostemon cablin* Benth. (16 mg), *Glycyrrhiza glabra* L. (6 mg), *Zingiberis officinale* Rosc (6 mg), *Ziziphus Jujuba* Mill. (10 mg)	Pill 200 mg	6-8 x 2-3 times a day	Take with lukewarm boiled water	For the treatment of ulcer, indigestion, gastro-intestinal weakness, discomfort in the chest and breast, vomiting, diarrhea and other intestinal disturbances
AA15	Hepaliv kapsul	*Paeomiae rubra* radix (200 mg), *Nothopanax scutellarium* Merr. (200 mg), *Pheretima* (300 mg), *Ligusticum chuanxiong* Hort. (140 mg), *Rhei* radix et rhizoma (300 mg), *Gentiana macrophylla* Pall. (400 mg), ***Clematis armandii*** **Franch.** (200 mg), *gardenia augusta* Merr. (260 mg	Capsule 500 mg	3 x 3 times a day, for 1 month		Helps to maintain a healthy liver, helps to cure fever

All collected samples were sealed in their original packaging before use and came in different forms such as liquid (1), powder (3), capsule (8) and pill (3). The preparation of the samples for analysis was done by collecting each sample (except the liquid sample) into a separate zip lock plastic sachet. The powder samples were put into the sachets directly, the capsule samples were opened first and only the content inside the capsule was put into the sachets and the pill samples were grinded with a mortar before the powder was collected in the sachets. AA14 has been grinded with a peppermill, since the structure was too strong for the mortar. Each sample in the zip lock plastic sachets was mixed manually to ensure the homogeneity. AA13 was homogenized in the original packaging, using a vortex mixer machine.

2.1.2 CHEMICALS

Dimethyl sulfoxide (DMSO), acetonitrile (ACN) and trifluoroacetic acid (TFA) are purchased from Merck, Germany. Mixture 1:1 AA-I and AA-II (≥ 97% purity) was purchased from Enzo, Life Sciences. Ultra-pure water was obtained from an Arium pro UF/VF water purification system (Sartorius Weighting Technology GmbH, Goettingen Germany). Methanol absolute ULC/MS was obtained from Biosolve, Valkenswaard the Netherlands.

2.1.3 METHANOL EXTRACTION

Methanol extracts were prepared by adding 1 g of the prepared sample to 10 ml of methanol, followed by sonication for 20 min at room temperature (RT). Then, the extracts were centrifuged for 15 minutes at 15000 rpm and 4°C and the supernatants of the extracts were collected to do an Ultra-Performance Liquid Chromatography (UPLC) analysis. The extraction and UPLC analysis were performed in 4 independent experiments. The accuracy of the method was assessed by choosing 1 sample from each form, AA1 (powder), AA10 (pill) and AA11 (capsule), and then to perform a linearity test using the weight per volume of methanol ratio concentrations at 2.5%, 5%, 10%, 20% and 40% each with an end concentration of 10 µM mixture 1:1 AA-I and AA-II. The linearity test was performed in 3 independent experiments. Because AA13 was the only liquid sample used in this study and showed positive results, no linearity test was performed for the liquid sample. The spiking was measured only once with AA6 and AA13 with the weight per volume of methanol ratio of 10% and an end concentration of 10 µM mixture 1:1 AA-I and AA-II. The mixture 1:1 AA-I and AA-II was added after methanol was added to the sample. For the rest, the linearity test and spiking were done with the same procedure as stated above. The percentage of recovery was used to correct the levels of AA in the samples with the following equations (Amersham Biosciences, 2004).

$$Factor\ \%\ of\ recovery\ = \frac{AA_m\ (\mu M)}{AA_S\ (\mu M)}$$

(Equation 1)

$$Level\ of\ AA\ in\ sample\ = \frac{AA_m\ (\mu M)}{factor\ \%\ of\ recovery}$$

(Equation 2)

In these equations, AA_m is the level of AA-I or AA-II that is measured and AA_s the amount of AA-I or AA-II that is added to the sample.

2.1.4 UPLC ANALYSIS

The analysis of the presence of AAs in Indonesian jamu was based on the methods described by Abdullah (2017), with minor modifications. To quantify the AA content in the samples of the Indonesian jamu, 3.5 µl per undiluted sample was analyzed by UPLC H-class (Acquitytm Waters), equipped with an acquity UPLC® BEH C18 1.7 µm x 2.1 x 50 mm column (Waters Ireland) with a sample temperature of 10°C and a column temperature of 40°C. A gradient was made with ultra-pure water containing 0.1% (v/v) TFA as solvent A and acetonitrile as solvent B. The flow rate was set on 0.6 ml/min and the starting condition was 80:20 (A:B), changing from 75:25 from 1 to 3 min, to 20:80 from 3 to 5 minutes and keeping the gradient at this condition for 1 minute. Then, the gradient was modified to 0:100 from 6 to 7.3 min, retained for another 0.2 min and then the starting conditions were reset from 7.5 to 8.5 min and kept at that level for 1 min to equilibrate the column. The detection was carried out by the Empower®3 software and chromatograms were analyzed at a wavelength of 224 nm for AA-I and 251 nm for AA-II. To be able to calculate the levels of AA in the tested samples, a calibration curve of AA-I and AA-II was made using the mixture 1:1 AA-I:AA-II. The calibration curve is measured in 3 independent experiments to get a more reliable result. The limit of detection (LoD) and limit of quantification (LoQ) were calculated with the following equations (ICH, 2005):

$$LoD = \frac{3.3\sigma}{S} \quad \text{(Equation 3)}$$

$$LoQ = \frac{10\sigma}{S} \quad \text{(Equation 4)}$$

In these equations, σ is the standard deviation of the intercept and S the slope, both obtained from the calibration curve. The LoD was calculated to be 0.9 µM for both AAs, the LoQ was calculated to be 2.8 µM for AA-I and 2.7 µM for AA-II.

2.1.5 ESTIMATED DAILY INTAKE (EDI) OF AAS PRESENT IN INDONESIAN JAMU

To evaluate the consumer risk for the intake of AA-I and AA-II in Indonesian jamu, the EDI was calculated based on the measured levels of AAs present in the samples, the recommended daily intake of the Indonesian jamu stated on the package (Table 1) and the average Indonesian adult body weight (bw) of 54 kg (Male 57.9 kg, female 50.1 kg) (FAO/WHO, 2014; FAO/WHO/UNU, 1981). For the intake, the highest recommended daily intake was chosen to be used for the calculation, assuming a lifetime daily intake. Furthermore, it was assumed that the prepared Indonesian jamu in its whole will be consumed.

In a previous study of Suparmi et al. (2018), three different exposure scenarios were considered to calculate the lifetime exposure of alkenylbenzenes. Two of these scenarios were used in the present study to determine the lifetime exposure of AA-I and AA-II. Scenario 1 was the calculation of the EDI for AA-I and AA-II individually, expressed in µg/kg/bw/day using the following equation:

$$EDI = \frac{Recommended\ daily\ intake\ (g) \times level\ of\ AA\ (\mu g/g)}{bw\ (54\ kg)}$$

(Equation 5)

For the samples that were found to be positive for both AA-I and AA-II, also the EDI for combined exposure was calculated. This was done by scenario 2, assuming that the potency of toxicity of AA-I and AA-II is equal using the following equation:

$$EDI = \frac{Recommended\ daily\ intake\ (g) \times\ (level\ of\ AA\text{-}I + AA\text{-}II)\ (\mu g/g)}{bw\ (54\ kg)}$$

(Equation 6)

Furthermore it was decided to calculate the EDI of the samples where AAs were not detected based on the LoD.

Due to several reasons it was decided to derive a $BMDL_{10}$ from AA-I which was used to calculate the MOE for both AA-I and AA-II and thus no relative potency of toxicity was taken into account. Firstly, AA-I is the most common AA in *Aristolochia* and *Asarum* plants and AA-II is, based on rodent studies, found to be less able to form DNA-adducts in comparison to AA-I in the liver (Dong et al., 2006; Mei et al., 2006; Shibutani et al., 2007). A second reason for this decision was that the costs of using AA-II in multiple experiments were too high.

2.2 Deriving points of departure by using the physiologically based kinetics modeling reverse dosimetry approach

All the protocols summed up in this chapter were obtained from the Toxicology Department of Wageningen University & Research.

2.2.1 General outline of the PBK modeling approach

In this study, physiologically based kinetic (PBK) modeling-facilitated reverse dosimetry was used to predict cytotoxicity and DNA-adduct formation in the human liver in vivo by translation of the in vitro concentration-response curves obtained with experimental work to in vivo dose-response curves. The combined in vitro-in silico PBK modeling approach to predict in vivo dose-response curves and a POD for risk assessment using in vitro cytotoxicity data was performed according to the following steps: 1. Establishment of in vitro concentration-response curves for the cytotoxicity of AA-I in HepG2 and HepaRG cells and DNA-adduct formation in HepG2 cells, 2. The development of a PBK model by describing the physiological, physiochemical and in vivo kinetic parameters of AA-I obtained by available literature data, 3. Evaluate the PBK model by comparing the outcomes of the model with available literature data, 4. Translation of the in vitro concentration-response curves into in vivo dose-response curves by applying the reverse dosimetry approach, 5. BMD analysis on the predicted in vivo dose-response data to obtain a POD for risk assessment and 6. Evaluation of the predicted POD against available literature (Abdullah, 2017).

2.2.2 ESTABLISHMENT OF IN VITRO CONCENTRATION-RESPONSE CURVES

2.2.2.1 Chemicals

HepG2 was obtained from the European Collection of Authenticated Cell Cultures (ECACC), Cat.nu. 85011430. HepaRG was obtained by the Toxicology Department, from Biopredic, November 2016. Williams E 12551-032, Penicilline/streptomycine (P/S) solution 15140-122, L-Glutamine 25030-024, Penicilline/streptomycine- and glutamine solution (PSG), and Trypsin-0.53 mM ethylenediminetetraacetic acid (EDTA) solution 15400-054 were obtained from Fisher Scientific. Phosphate-buffered saline (PBS) and Eagle's minimal essential medium (EMEM) were obtained from Gibco, Paisley UK. Non-essential amino acids (NEAA) were obtained from Invitrogen, Breda, The Netherlands. DNA mini kit was purchased from Qiagen, Hilden, Germany. Ultra-pure water was obtained from an Arium pro UF/VF water purification system (Sartorius Weighting Technology GmbH, Goettingen Germany). AA-I powder, Fetal Calf Serum (FCS), DMSO, ACN, human insulin, hydrocortisone-21-hemisuccinate, spleen phosphodiesterase (SPDE), venom phosphodiesterase (VPDE) , nuclease P1 and alkaline phosphatase were purchased from Sigma-Aldrich (now Merck).

2.2.2.2 Cell culture

For the HepG2 cells, the 'Culture protocol HepG2 cells (Jac Aarts)' was used with minor modifications. The cells were cultured in 75cm^2 flasks in 12 ml growth medium EMEM+++ (1% PSG, 1% NEAA and 10% FCS). The growth medium was refreshed 2 times a week until they were 85-95% confluence. Then, the cells were washed twice, once with 10 ml PBS and once with 6 ml PBS and 1 ml trypsin (0.53 mM EDTA solution). Hereafter, 2.5 ml trypsin was added for 10 seconds, 1.5 ml trypsin was discarded and the flasks were put in the incubator for 10 minutes for the cells to detach. The flasks were treated gently with no hitting or shaking to avoid clumping of cells. After trypsinizing, the cells were re-suspended with 10 ml of growth medium and sub-cultured by bringing a 3-4 dilution of the cell suspension in a new flask, complemented with growth medium until 12 ml was reached and placed in the CO_2-incubator at 37° C.

For the HepaRG cells, the 'HepaRG® Cell line culture Maintaining & culture support production "Normal Density" process, Instruction manual' together with the 'Culture protocol HepaRG cells' were used to culture the cells. In short, the cells were cultured in 25 cm^2 flasks in 5 ml growth medium Williams E++++ (10% FCS, 1% P/S, 1% L-glutamine, 0.05% human insulin and 1% hydrocortisone-21-hemisuccinate) for two weeks. The medium was refreshed every 2-3 days. Hereafter, the cells were washed twice with 5 ml PBS and after removing the PBS trypsinized with 1.2 ml trypsin for 5 minutes to detach the cells. Then, 5 ml of growth medium was again added to the flask to re-suspend the cells and the cells were counted with the Cellometer using 0.05% Tryptan Blue solution. For sub-culturing in 25 cm^2 flasks, 5 * 10^5 cells per 5 ml were added to the flask. For seeding, the cells were diluted until the amount of 0.9 * 10^5 cells/ml was reached to seed the cells in the 96-wells plates. The 60 inner wells were filled with 100 µl cell suspension, the 36 outer wells were filled with 100 µl PBS. The cells were then cultured for another two weeks in growth medium and afterwards two more weeks in differentiation medium (for the first 2-3 days growth medium + 1% DMSO, then growth medium + 1.7% DMSO). The medium was refreshed every 2-3 days. After two weeks of treatment with the exposure medium, the cells were completely differentiated and used to perform the WST-1 assay.

2.2.2.3 WST-1 assay

The WST-1 assay was carried out by following the 'MTT/WST1 protocol' and was performed to determine the cytotoxicity of HepG2 and HepaRG cells upon exposure of AA-I at different levels. The HepG2 cells were collected from the flask by trypsinizing and re-suspended with growth medium until there were 5 x 10^5 cells/ml. Then, 100 µl of cell suspension was seeded in the 60 inner wells of the 96-wells plate and the 36 outer wells were filled with 100 µl PBS. For the HepaRG cells, the seeding and culturing before carrying out the WST-1 assay is stated in the section 'cell culture'. After incubating the 96-wells plates for 24 hours at 37° C, 5% CO_2 and 100% humidity, the exposure medium was added to the wells. Both HepG2 and HepaRG cells were incubated with exposure medium either with and without FCS in the end concentrations of 0, 0.1, 0.3, 1, 3, 10, 30, 100 and 300 µM AA-I (0.5% DMSO). After another 24 hours, 5 µl WST-1 solution was added to each well and the absorbance at 440 nm and 620 nm was measured after 2 hours using the Spectramax® iD3 reader using Softmax Pro Software 7.0.2. Triton X-100 was used as positive control and DMSO as solvent control. Each concentration was tested six times per experiment and three independent experiments were performed per type of incubation and cell line. The data was analyzed by calculating the formazan extinction by subtracting the 620 nm absorbance signal from the 440 nm, setting the average of the solvent control at 100% to all other exposures and then calculating the average per exposure level.

2.2.2.4 DNA-adduct assay

The in vitro testing of DNA-adduct formation was based on the methods described by Abdullah (2017) with minor modifications. The exposure medium consisted of the end concentrations of 0, 0.3, 1, 3, 10, 30 µM AA-I (0.5% DMSO) in EMEM++ (PSG and NEAA) without FCS. The exposure of the different concentrations was done in 75cm^2 flasks for 24 hours at a confluence of 80-90%. After exposure, the cells were collected and lysed according to the protocol 'DNA isolation (cells)'. The cells were washed with PBS and trypsinized as stated before, collected in 10 ml PBS, collected in a 10 ml tube and centrifuged at 1500 rpm for 5 min at RT. Hereafter the supernatant was removed and the pellet was re-suspended in 1.2 ml PBS and transferred to a 1.5 ml Eppendorf tube. To lyse the cells, the re-suspended pellet was again centrifuged at 1500 rpm for 5 minutes at RT, the supernatant removed, re-suspended in 500 µl PBS, centrifuged at 1500 rpm for 5 minutes at RT, the supernatant removed and 200 µl RTL buffer (DNA mini kit) added and vortexed until the suspension was clear. The lysed samples were stored at -20° C until DNA isolation.

2.2.2.5 DNA isolation and digestion

The protocol 'DNA isolation (cells)' was used for DNA isolation with minor modifications. All centrifuge steps were performed at 20000 g at RT and after each centrifuge step the filter was placed in a new centrifugation tube unless stated otherwise. Shortly, the lysed samples were adjusted to RT and 20 µl Proteinase K and 200 µl AL buffer were added, vortexed for 15 seconds and spun down. Then, the samples were incubated at 56°C for 10 minutes and spun down. 200 µl EtOH (100%) was added and the samples were vortexed for 15 seconds, followed by a spin down. Hereafter, 4 µl RNase A was added and the lysate was transferred to a DNA isolation filter in a centrifugation tube and incubated for 15 min at RT. After the incubation time, the lysate was centrifuged and 500 µl AW1 buffer was added, centrifuged again, 500 µl AW2 buffer was added and centrifuged again. Finally, 200 µl H_2O (Millipore)

was added, the sample was incubated for 10 minutes at RT and centrifuged and the supernatant in the centrifugation tube was put on ice to use the sample for determining the yield and purity of the extracted double-stranded DNA with the Nano drop 1000 technology. This was determined by measuring the absorbance ratio of A260/280 and A260/230 where a ratio of ~1.8 and 2.0-2.2 were considered pure (Scientific, 2013). Hereafter the samples were stored at -80° before DNA digestion.

The digestion of DNA was performed using the protocol 'DNA Digestion'. All working steps were performed while the samples were on ice. In short, 40 µl P1 buffer (300 mM sodium acetate, 1 mM $ZnSO_4$, pH 5.3), 20 µl SPDE solution (0.0004 U/ µl) and 10 µl nuclease P1 (0.5U/ µl in water) were added to 30 µl DNA (max. total 50 µg), vortexed, spun down and incubated for 4 hours at 37° C. Then, 40 µl PA buffer (500 mM Tris, 1 mM EDTA, pH 8.0), 20 µl VPDE (0.00026 U/ µl in water) and 1.6 µl alkaline phosphatase (0.27 U/µl) were added to the DNA, vortexed, spun down and the sample was incubated again for 2 hours at 37° C. The hydrolyzed samples were evaporated to dryness and reconstituted in 50 µl H_2O (Millipore). The samples were kept in UPLC vials at -80°C until analysis using the Triple Quadrupole Liquid Chromatography Mass Spectrometer (LC-MS/MS). To obtain a calibration curve, frozen synthesized dA-AA-I and dG-AA-I, previously used by Abdullah (2017), were defrosted and measured in the LC-MS/MS.

2.2.2.6 LC-MS/MS analysis

The LC-MS/MS analysis was performed on a Nexera X2 Ultra High Performance Liquid Chromatography (UHPLC) system coupled to an MS (MS-8040; Shimadzu Benelux, 's Hertogenbosch, The Netherlands). In short, 5 µl of sample was injected onto a Phenomenex Kinetex-C18 column, 50 x 2.1 mm, 1.7 µm (Utrecht, The Netherlands), with a Phenomenex Security Guard ULTRA pre-column with a sample temperature of 10°C and a column temperature of 40°C. A gradient was made with ultra-pure water containing 0.1% v/v formic acid as solvent A and 100% ACN containing 0.1% (v/v) formic acid as solvent B. the flow rate was set at 0.3 ml/min. The starting condition was 95:5 (A:B) for 1 min, followed by changing to 0:100 in 6 min and remaining 0:100 for 0.5 min. Then it went back to 95:5 in 0.1 min and kept in this condition for 4.4 min so the column could re-equilibrate at 40°C. The analysis of a sample took 12 min in total. The mass spectrometric analysis in the positive ion mode was optimized with the following settings: nebulizer gas flow at 2 l/min, drying gas flow at 15 l/min, DL temperature of 250°C, heat block temperature at 400°C and CID gas at 230 kPa. The dwell time per transition was 33msec. A divert valve was used in order to discard the eluate in the first min (e.g. removal of salts) and after finishing MS measurement. The operation was in MRM mode with the m/z transitions of 543 → 427 for dA-AA-I and 559 → 443 for dG-AA-I. The collision energy used to obtain the daughter fragments was 20 eV for dA-AA-I and 28 eV for dG-AA-I. The analysis was done by calculating the amount of dA-AA-I and dG-AA-I per 10^8 nts in pmol.

2.2.3 COMPARTMENTS AND PARAMETERS OF THE PBK MODEL

All parameters used were previously reported by Abdullah (2017). A schematic diagram (Figure 3) was produced to show the structure of the PBK model. The model consists of a separate compartment for the liver as metabolizing organ, the kidney as excretion organ, GI-tract as uptake organ, slowly perfused tissue, rapidly perfused tissue, fat tissue and blood. It is known that the liver is the primary organ responsible for the metabolism of AA-I, but also in the kidney metabolism takes place (Marie

Stiborová et al., 2008). However, in this study the metabolism of the kidney is excluded since the lack of available data. Furthermore, since the toxicity of AA-I is determined by bioactivation in the human body itself, it implies that the maximum concentration (C_{max}) of AA-I itself is the parameter that forms the basis for the in vitro to in vivo extrapolation. This means that the PBK model should adequately predict the kinetics of disappearance of AA-I (Abdullah, 2017). The kinetic data of the detoxification of AA-I by its conversion into AA-Ia was reported to be a V_{max} of AA-Ia 0.02 ± 0.0 nmol/min/mg protein in tissue fraction and a K_m of 58.4 ± 11.1 µM. The conversion of AA-I to AA-Ia is the major metabolic pathway for predicting the C_{max} for AA-I. Other minor metabolic pathways such as bioactivation by nitroreduction, although a really important factor for carcinogenicity, has no significant influence on the predicted C_{max} for AA-I (Abdullah, 2017). Upon oral exposure, it was assumed that AA-I was taken up by the GI-tract and absorbed by the liver. No absorption rate constant (ka) is known for humans. In the literature a ka of 3.27 h^{-1} is reported for rats (Su et al., 2004). For beagle dogs a ka of 1.88 – 3.13 h^{-1} was reported (Yang et al., 2011), which is quite similar to the ka reported for rats. Abdullah (2017) reported that the overall catalytic efficiency (V_{max}/K_m) for metabolic conversion of AA-I by rat and human liver was comparable, therefore it is decided to use the ka of 3.27 h^{-1}, reported for rat. Furthermore, no allometric scaling of the ka is done since the permeability of compounds across the intestinal barrier of different species is relatively constant (Sharma & McNeill, 2009).

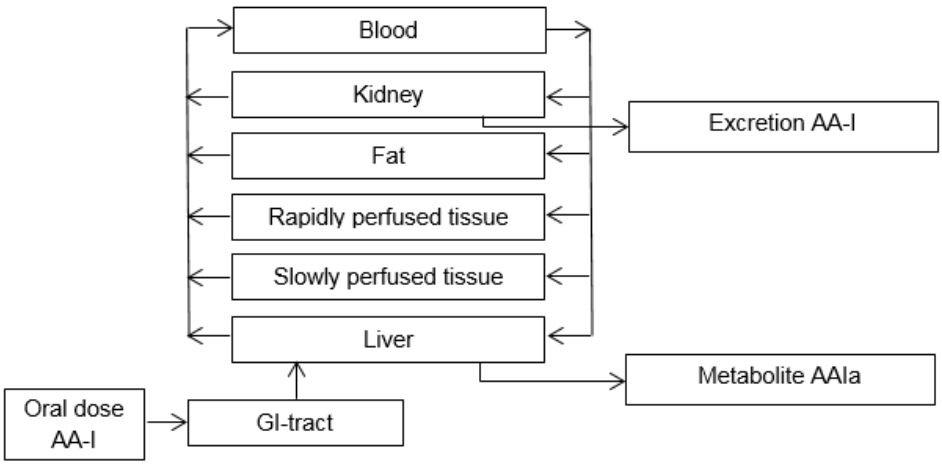

Figure 3: Schematic diagram of relevant compartments included in the PBK model

For running the PBK model, the physiological parameters of tissue volumes and blood flow rates were obtained from Brown et al. (1997). For the blood flow rates, it is crucial that the sum is exactly 100% of the cardiac output, otherwise the outcomes of the model typically leads to severe inaccuracy and model failure. The physicochemical parameters, the partition coefficients, were calculated based on the log K_{ow} using the method described by Berezhkovskiy (2004). The log K_{ow} of AA-I was reported to be 4.45 ± 0.07, meaning that AA-I is a lipophilic compound (Han et al., 2012). Furthermore the scaling of the V_{max} was carried out by correcting for a content of 143 mg microsomes/g liver (Punt et al., 2008), a liver weight calculated by the PBK-model (1.8 kg) and converting units to get the V_{max} of AA-Ia in µmol/hr. The K_m obtained in vitro is assumed to be of the same value in vivo. The biliary and urinary

excretion rate constants were scaled to 26.8 and 0.1 h^{-1}, using allometric scaling from rat to human by Abdullah (2017), using the data from Ren et al. (2014).

2.2.4 PBK MODEL OUTCOME AND EVALUATION

The mathematical equations of the PBK model were solved with the Berkeley Madonna software, using the Rosebrock (stiff) method. To evaluate the PBK model on the accuracy of predicting the concentration of AA-I in the blood of a human body, the outcome of the model should be compared to pharmacokinetic human in vivo data. In a study on humans which were treated with a daily dose of 0.9 mg AAs for three days, aristolactam I and II were identified in the urine. In another study, aristolochic-like substances were detected at relatively high concentrations in the bile, urine, cerebrospinal fluid and saliva in humans treated with 1.35 mg AA-I for three days (EMEA, 1997). Unfortunately detailed data such as percentage of excretion or amount of AA-I and/or metabolites detected were not reported and therefore cannot be used to evaluate the PBK model. Therefore, the model compared three types of intake levels, one intake level as obtained by the UPLC analysis, one intake level based on the literature and one assumed maximum intake level based on the findings of the UPLC analysis and the literature.

To determine the sensitivity of the parameters a sensitivity analysis was performed. Normalized sensitivity coefficients (SC) were calculated using the following equation:

$$SC = (C' - C)/(P' - P) \times (P/C)$$

(Equation 7)

Where C is the initial value of the model output (C_{max}), C' is the modified value of the model output after changing the parameter, where P is the initial parameter value of the model and P' is the modified parameter value. A SC of >0.1 was considered to be significantly sensitive. The analysis was done using a 5% change in each individual parameter, where only one parameter at the time was changed (Rietjens et al., 2011). For testing the sensitivity for blood flow parameters, since this has to be 100% in the model at all times, the change of one blood flow parameter was corrected by also changing the blood flow of the slowly perfused tissue. When the blood flow of the slowly perfused tissue parameter was changed, the correction was done by also changing the blood flow of the richly perfused tissue.

2.2.5 TRANSLATION OF THE IN VITRO CONCENTRATION-RESPONSE CURVES TO IN VIVO DOSE-RESPONSE CURVES USING REVERSE DOSIMETRY APPROACH

With the concentration-response curves obtained from the cytotoxicity and DNA-adduct assays, in vivo dose-response curves were predicted by using the PBK model-based reverse dosimetry approach. For this translation, the data from the concentration-response curves were corrected for the fraction unbound (F_{ub}) in vitro and in vivo. After this correction, the concentration unbound (C_{ub}) could be determined in vitro and in vivo. The F_{ub} and C_{ub} were calculated using the following equations (J. Wu et al., 2012):

$$f_{ub} = \frac{1}{1 + nKaP}$$

(Equation 8)

$$C_{ub} in\ vitro = C_{test} \times f_{ub} in\ vitro$$

(Equation 9)

$$C_{ub} in\ vivo = C_{max} \times f_{ub} in\ vivo$$

(Equation 10)

Where in equation 8 n is the number of binding sites, Ka is the binding constant and P the concentration of proteins in the plasma. In this study, n = 1.017 and Ka = 288700 M as reported by X. Wu et al. (2011) and P in vitro = 36 µM and P in vivo = 600 µM as reported by Gülden and Seibert (2003) were used to solve equation 8. For equation 9, C_{ub} in vitro is the unbound in vitro concentration of AA-I, C_{test} is the total concentration level tested for AA-I and F_{ub} is the unbound fraction of AA-I in vitro. For equation 10, C_{ub} in vivo is the unbound in vivo concentration of AA-I, C_{max} is the maximum blood concentration of AA-I upon an oral dose and F_{ub} is the unbound fraction of AA-I in vivo. The oral dose was predicted by setting each C_{max} as found by correcting the exposed amount of AA-I (µM) for the F_{ub} in vitro and F_{ub} in vivo equal to the C_{max} of AA-I in the liver tissue as calculated by Berkeley Madonna software using the Rosebrock (stiff) method.

2.2.6 BMD ANALYSIS OF THE PREDICTED IN VIVO DOSE-RESPONSE DATA

BMD modeling was applied on the predicted in vivo dose-response data to derive a $BMDL_{10}$ value for cytotoxicity and DNA-adduct formation in the human liver. The BMD calculated the quantal response including litter effect using the EFSA Statistical Models software, benchmark dose modeling using the default settings.

2.3 RISK ASSESSMENT OF AAS IN INDONESIAN JAMU USING THE MARGIN OF EXPOSURE (MOE) APPROACH

The MOE values were determined by dividing the $BMDL_{10}$ by the EDI using the following equation:

$$MOE = \frac{BMDL_{10}\ (\mu g/kg\ bw)}{EDI\ (\mu g/kg\ bw)}$$

(Equation 11)

The MOE was calculated for the cytotoxicity in the human liver based on the calculated EDI of AA-I and AA-II individually and for the combined exposure while assuming equal potency of toxicity using the lowest derived $BMDL_{10}$. Since the cytotoxicity assay assessed a non-carcinogenic effect, a MOE value of 100 or higher is considered to be of low concern for human health.

3. RESULTS

3.1 PRESENCE AND LEVELS OF AAS IN INDONESIAN JAMU

3.1.1 UPLC ANALYSIS

The UPLC analysis was carried out to see whether AAs were present in Indonesian jamu and thus if there was a reason to perform an associated risk assessment. In the chromatogram obtained by the UPLC, AA-I eluted in between 6.90 – 6.95 min and AA-II in between 6.84 – 6.91 min. The levels of the AAs were calculated based on the obtained calibration curves for AA-I (R^2 0.9967) and AA-II (R^2 0.9971) and corrected with the percentage of recovery for the different forms of samples. The average percentage of recovery of AA-I and AA-II based on the linearity test was 0 and 0% for powder (AA1), 6.7% and 21.8% for pill (AA10) and 36.6% and 67.7% for capsule (AA11) respectively. Since the percentages of recovery for the pill sample were lower than the recovery results of the spiking for AA6 and because no linearity test was performed for the liquid sample (AA13) it was chosen to correct AA6 and AA13 with the percentages of recovery of the spiked samples which were 54.4% and 45.8% for AA-I and 49.1% and 95.2% for AA-II respectively.

The analysis of the UPLC showed that two out of 15 samples were found positive for the presence of AAs, where AA6 (pill) was found to be positive for both AA-I and AA-II (Figure 4) and AA13 (liquid) was found positive only for AA-II (Table 2). In AA6, AA-I was over a 2-fold higher than AA-II namely 21.6 µg/g AA-I and 9.6 µg/g AA-II. In AA13, 10.5 µg/g AA-II was found to be present. According to the information found on the package of the Indonesian jamu and/or the database of KNApSAcK family of Afendi et al. (2011), both positive samples were suspected to contain the same toxic botanical, *Aristolochia debilis*, commonly known as Dutchman's pipe or Birthwort. To exemplify, AA6 contains the suspected botanical *Aristolochia debile* Sieb.Et.Zucc., which is known to contain aristolochic acid and AA13 claims to contain *Saussurea lappa* which itself does not contain aristolochic acid but *Saussurea lappa* has the same Pin Yin name as *Aristolochia debilis* and therefore is suspected to be mixed-up or adulterated (Anderson & Vlietinck, 2000; IARC et al., 2002).

In the other 13 samples no AAs were detected with the UPLC analysis. For these samples, the LoD, 0.9 µM for both AAs, were used and corrected with the percentage of recovery obtained from the linearity test to calculate the EDI.

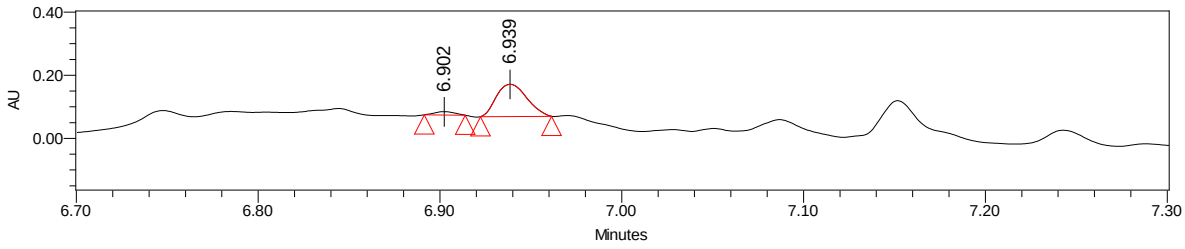

Figure 4: Chromatogram of the methanol extract (exp. 2) of AA6 obtained at a wavelength of 224 nm. Left: retention time 6.902 AA-II. Right: retention time 6.939 AA-I.

Table 2: Presence of AAs in Indonesian jamu and the EDI calculated based on the recommended daily intake and the average Indonesian bodyweight

Sample No.	AA present (µg/g)[a,c]		EDI (µg/kg bw/day)[b,c]	
	AA-I	AA-II	AA-I	AA-II
AA1	nd[d]	nd	0.8	0.7
AA2	nd	nd	0.3	0.3
AA3	nd	nd	0.3	0.3
AA4	nd	nd	0.3	0.1
AA5	nd	nd	0.5	0.2
AA6	21.6 ± 6.0	9.6 ± 12.4	1. 4 ± 0.4	0.6 ± 0.8
AA7	nd	nd	0.5	0.2
AA8	nd	nd	0.4	0.2
AA9	nd	nd	0.5	0.2
AA10	nd	nd	4.0	1.1
AA11	nd	nd	0.5	0.2
AA12	nd	nd	0.5	0.2
AA13	nd	10.5 ± 1.9	0.6	1.0 ± 0.2
AA14	nd	nd	4.2	1.1
AA15	nd	nd	0.7	0.3

[a] Mean of 4 independent experiments

[b] EDI of the non-detected samples were calculated using the LoD of 0.9 µM for AA-I and AA-II

[c] Levels of AA were corrected by the percentage of recovery

[d] Not detected

3.1.2 ESTIMATED DAILY INTAKE

The EDIs were calculated based on the level of AA present in the Indonesian jamu, assuming that the intake of the samples was equal to the recommended daily intake (see materials and methods, Table 1) with a bodyweight of 54 kg. The combined exposure of AA-I and AA-II was done by adding up the levels of the AAs in µg/g that was found in the Indonesian jamu. In this combined exposure, equal potency of toxicity was assumed.

The EDI for AA6 was 1.4 µg/kg bw/day for AA-I, 0.6 µg/kg bw/day for AA-II and 2.0 µg/kg bw/day for the combined exposure. For AA13 the EDI was 1.0 µg/kg bw/day for AA-II with a combined exposure of 1.6 µg/kg bw/day, using the LoD for calculating the possible level of AA-I in the Indonesian jamu. For the negative samples, the EDI values for the individual AAs ranged in between 0.3 and 4.2 µg/kg bw/day for AA-I and in between 0.1 and 1.1 µg/kg bw/day for AA-II. For the combined exposure, the EDI for the negative samples ranged in between 0.4 and 5.4 µg/kg bw/day.

3.2 IN VITRO CONCENTRATION-RESPONSE CURVES

3.2.1 CYTOTOXICITY ASSAY

The concentration-response curves of the cytotoxicity HepG2 and HepaRG cells in vitro upon AA-I exposure are displayed in Figure 5. The IC_{10} for HepG2 incubated with and without FCS was determined to be 106.1 and 5.8 µM respectively. HepaRG cells incubated with and without FCS showed an IC_{10} of 11.7 and 0.1 µM respectively (Table 3).

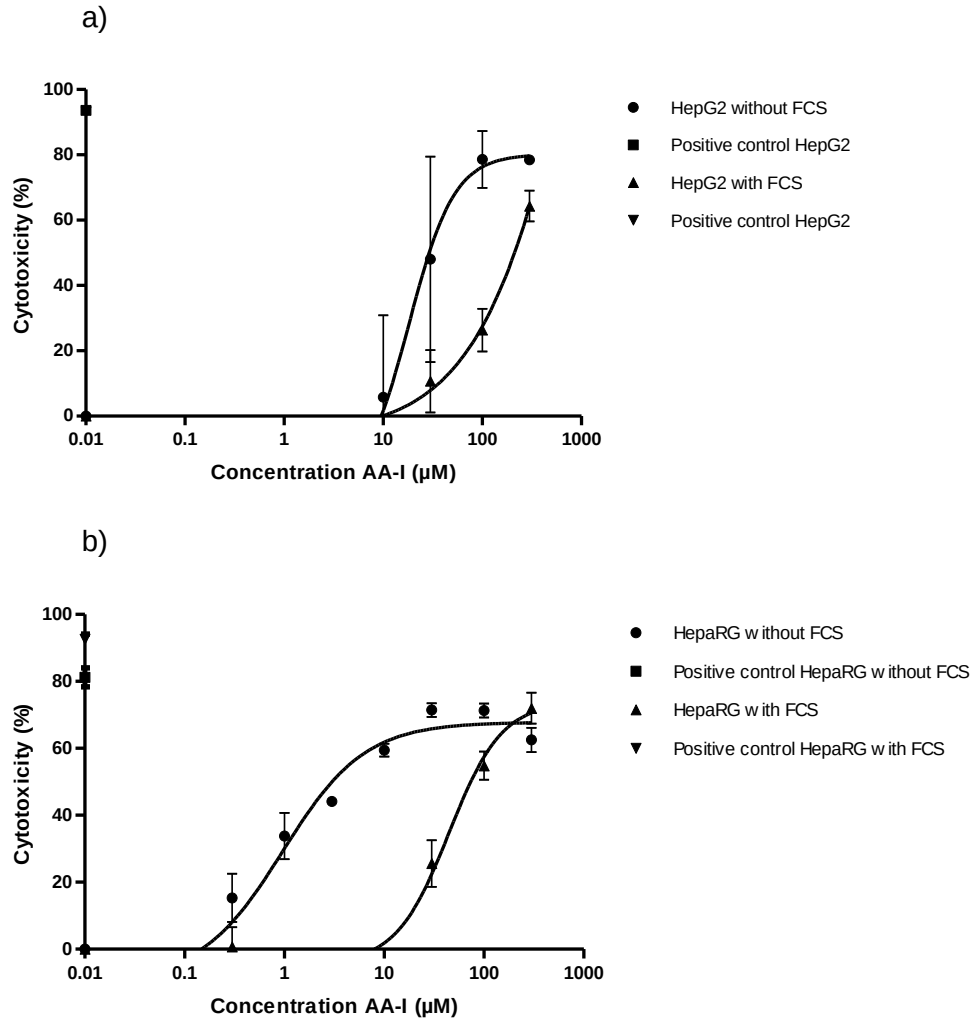

Figure 5: Concentration-response curves for the cytotoxicity of HepG2 (a) and HepaRG (b) cells incubated with and without FCS upon AA-I exposure based on a 24 hour exposure (mean values ± SD of 3 independent experiments).

Table 3: Cytotoxicity of AA in HepG2 and HepaRG cells expressed in IC_{10}

Cell line	HepG2 without FCS	HepG2 with FCS	HepaRG without FCS	HepaRG with FCS
IC_{10} (µM)	5.8	106.1	0.1	11.7

3.2.2 DNA-ADDUCT ASSAY

The formation of DNA-adducts upon exposure of AA-I was assessed for HepG2 cells incubated without FCS only. The detection limit for calculating dA-AA-I and dG-AA-I was 0.25 nM based on the given information that an ionic count, performed by the LC-MS/MS, below 150 gives unreliable results and therefore cannot be used. The elution was 6.07 min for dA-AA-I and 5.59 min for dG-AA-I. The synthesis of the adducts resulted in a very low percentage of recovery, 0.04% for dA-AA-I and 1.47% for dG-AA-I. These percentages were used to correct the amount of µM in the calibration curve for dA-AA-I and dG-AA-I and then the calibration curve was used to calculate the amount of adducts in the samples.

After a 24 hour exposure, no adducts were detected in HepG2 cells exposed to 0, 0.3, 1 or 3 µM AA-I. When exposed to 10 µM AA-I, 52.4 pmol dA-AA-I per 10^8 pmol nts were detected (Figure 6) whereas for dG no adducts of AA-I were detected. Upon an exposure level of 30 µM AA-I, 325.4 pmol dA-AA-I and 10.0 pmol dG-AA-I per 10^8 pmol nts were detected.

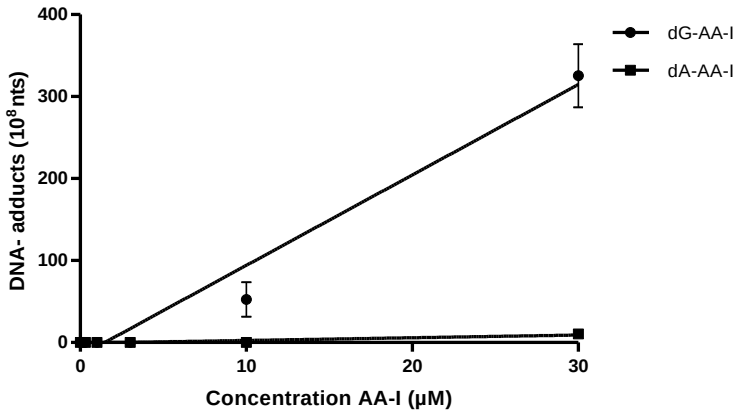

Figure 6: Concentration-response curves for dA-AA-I and dG-AA-I in HepG2 cells incubated without FCS based on a 24 hour exposure (mean values ± SD of 3 independent experiments).

3.3 PBK MODEL OUTCOME AND COMPARISON

Because of the lack of kinetic in vivo data in humans, it was decided to show the PBK model outcome comparing three intake levels of AAs. Based on the UPLC analysis of Indonesian jamu on the presence of AAs, the concentration level of AA-I in the liver tissue was shown for an oral intake of 1 µg/kg bw day, which was the lowest EDI calculated from the positive samples (Figure 7). At this intake level, a C_{max} of 0.02 µM was observed. Then, retrospective examination of the prescriptions done by Joëlle L Nortier et al. (2003) confirmed that a Belgium AAN patient took an accumulative dose of approximately 189 grams of *Aristolochia fangchi* in the 14 months that she took slimming pills. This is calculated to be 6.5 mg/kg bw per day assuming that the pills were taken daily over the whole period. A single oral dose of 6.5 mg/kg bw leads to a C_{max} of 63.8 µM. Lastly, based on the calculated daily intake of 6.5 mg/kg bw per day and given that the most important way of ingestion of AAs are via traditional herbal medicines or adulterated slimming pills, a maximum intake of 10 mg/kg bw was assumed. The assumed maximum intake level showed a C_{max} of 98.2 µM as predicted by the PBK model.

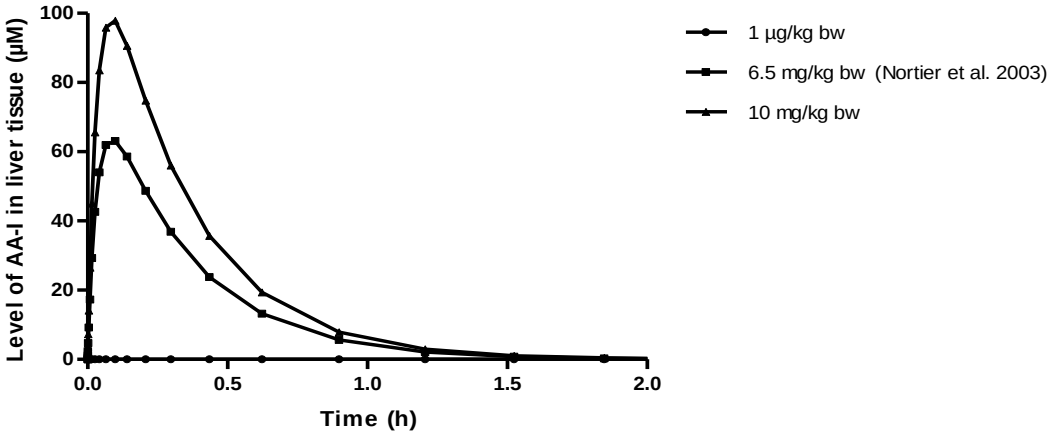

Figure 7: Comparison of three different exposure levels of AA-I upon a single oral dose based on the UPLC analysis (1 µg/kg bw), data from Joëlle L Nortier et al. (2003) (6.5 mg/kg bw) and an assumed maximum intake (10 mg/kg bw).

3.4 SENSITIVITY ANALYSIS

The sensitivity analysis was performed to determine whether individual parameters had a significant influence on the model outcome. The influence of the parameter was reported as significantly sensitive when the SC was >0.1 which was the case for the volume of the liver (VLc), the absorption rate constant (ka) and the biliary excretion rate constant (kbile) (Figure 8). Most parameters didn't have any influence on the model outcome of the level of AA-I in the liver. This can be explained by the fact that the liver is, besides the GI-tract where AA-I is taken up, the first organ that AA-I will reach.

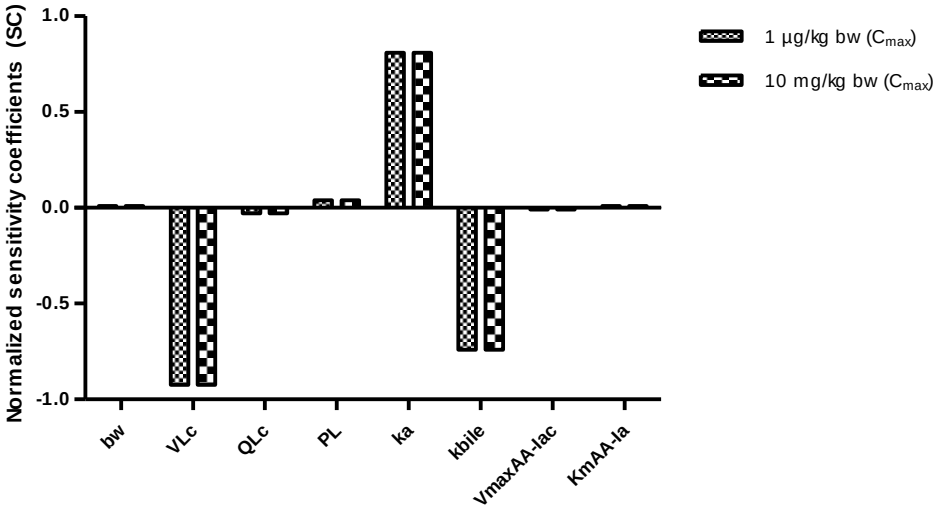

Figure 8: Normalized sensitivity coefficients (SC) for the C_{max} in liver tissue based on a single oral dose of 1 µg/kg bw and 10 mg/kg bw. All parameters that gave a response are presented, parameters with a SC of >0.1 were considered significantly sensitive. bw = bodyweight, VLc = volume of liver, QLc = blood flow of liver, PL = partition coefficient of liver, ka = absorption rate constant, kbile = biliary excretion rate constant, VmaxAA-Iac and KmAA-Ia = maximum rate of formation and the Michaelis-Menten constant for formation of AA-Ia by the liver.

3.5 TRANSLATION OF IN VITRO CONCENTRATION-RESPONSE CURVES TO IN VIVO DOSE RESPONSE CURVES USING THE REVERSE DOSIMETRY APPROACH

The dose-response curves of the cytotoxicity and the DNA-adduct formation were obtained by setting the in vitro exposed concentration level of AA-I as corrected for the f_{ub} in vitro and in vivo equal to the C_{max} as found by the Berkeley Madonna software to determine the oral dose (figure 9, 10). The f_{ub} in vitro was calculated to be 0.0864 and 1 for the cells incubated with and without FCS respectively and the f_{ub} in vivo was calculated to be 0.0056. After these corrections were applied, it was expected that the dose-response curves of the same cell line with the different incubations were the same. This is however not the case which indicates that different results will be obtained when using different incubation techniques.

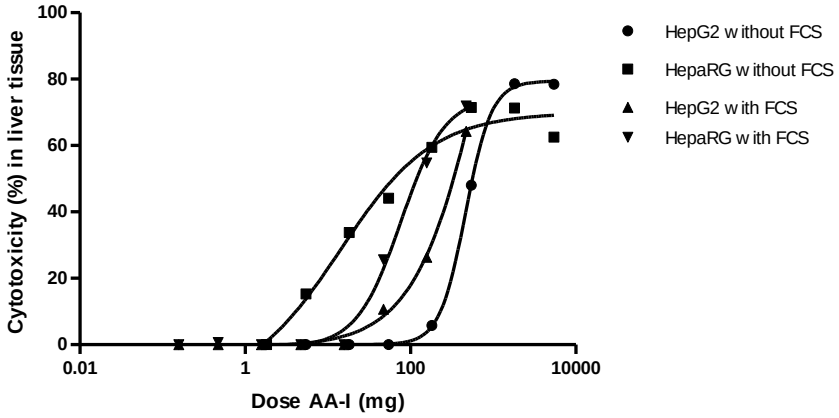

Figure 9: Dose-response curves as predicted by the PBK model for acute liver cytotoxicity of HepG2 and HepaRG cells upon oral intake of AA-I.

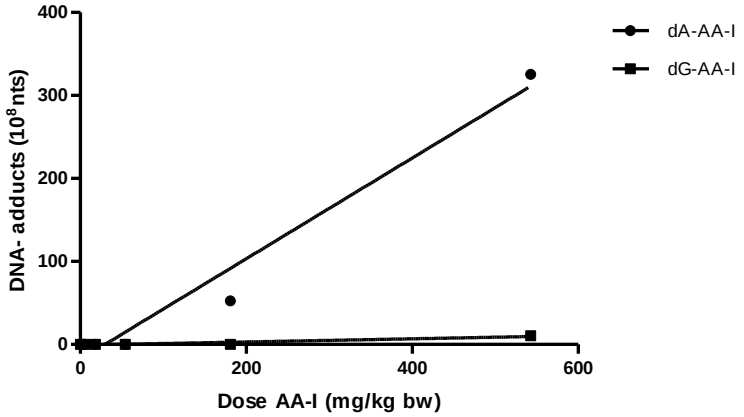

Figure 10: Dose-response curves as predicted by the PBK model for the formation of dA-AA-I and dG-AA-I upon oral intake of AA-I.

3.6 BMD ANALYSIS OF THE PREDICTED DOSE-RESPONSE CURVES

The calculated $BMDL_{10,}$ based on the predicted dose-response curves for cytotoxicity and DNA-adduct formation, can be found in Table 4. $BMDL_{10}$ values for acute liver cytotoxicity based on the HepG2 cells were calculated to be 49.7 - 187 mg/kg bw day. For the HepaRG cells the $BMDL_{10}$ values for cytotoxicity were calculated to be 2.66 – 27.5 mg/kg bw day. The $BMDL_{10}$ value for the dA-AA-I formation was calculated to be 90.5 mg/kg bw.

Table 4: $BMDL_{10}$ values (mg/kg bw) for cytotoxicity and dA-AA-I

Cell line	Cytotoxicity HepG2 without FCS	Cytotoxicity HepG2 with FCS	Cytotoxicity HepaRG without FCS	Cytotoxicity HepaRG with FCS	dA-AA-I
$BMDL_{10}$ (mg/kg bw)	187	49.7	2.66	27.5	90.5

3.7 RISK ASSESSMENT OF INDONESIAN JAMU USING THE MOE APPROACH

The risk assessment of Indonesian jamu was carried out to determine whether the intake of AAs via Indonesian jamu was a priority for risk management. In this step, equal potency of toxicity of AA-I and AA-II was assumed. Furthermore, because the lowest $BMDL_{10}$ value as calculated for the liver cytotoxicity was over a 30-fold lower than the $BMDL_{10}$ value as calculated for dA-AA-I formation, it was decided to only perform the risk assessment for the cytotoxicity based on the lowest derived $BMDL_{10}$ value of 2.66 mg/kg bw day. To compare the liver cytotoxicity to the target organ, the risk assessment was also carried out for kidney cytotoxicity. The $BMDL_{10}$ for the kidney cytotoxicity was derived using the same PBK model and was reported by Abdullah (2017) to be 0.5 mg/kg bw based on the data of Huljic et al. (2008). For the samples where no AAs were detected, the MOE values were calculated based on the LoD of 0.9 µM for AA-I and AA-II.

The MOE values are shown individually as AA-I and AA-II and as combined exposure (Figure 11). The risk assessment for the liver cytotoxicity showed that all MOE values were above 100, both for the AAs individually and as combined exposure. For the kidney cytotoxicity, all individual exposure levels showed MOE values above the threshold of 100. When taking into account combined exposure, AA10 (99.5) and AA14 (93.4) had MOE values below the threshold of 100, which indicate a priority for risk management. Furthermore, the MOE values for the kidney cytotoxicity were found to be a 5-fold lower as compared to the MOE values for the liver cytotoxicity.

a)

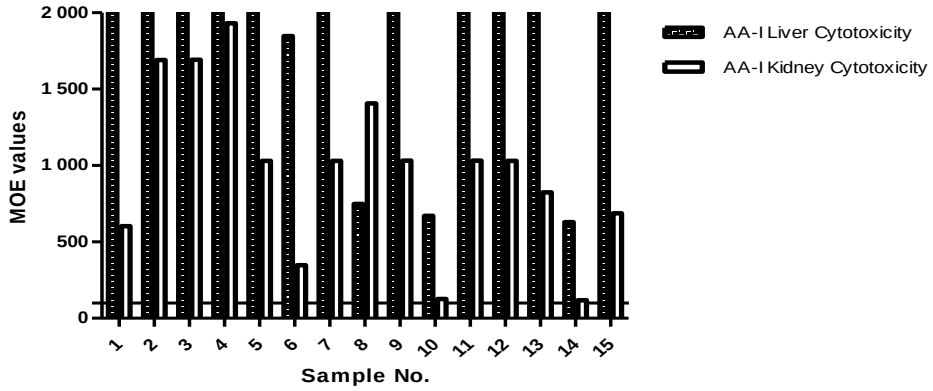

b)

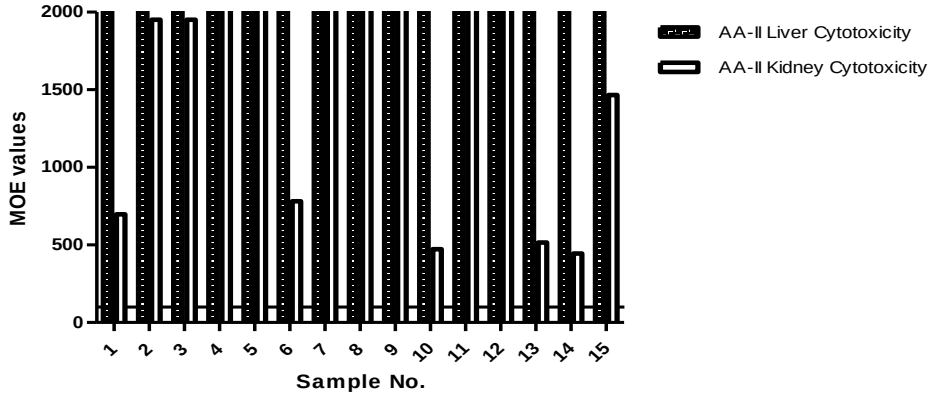

c)

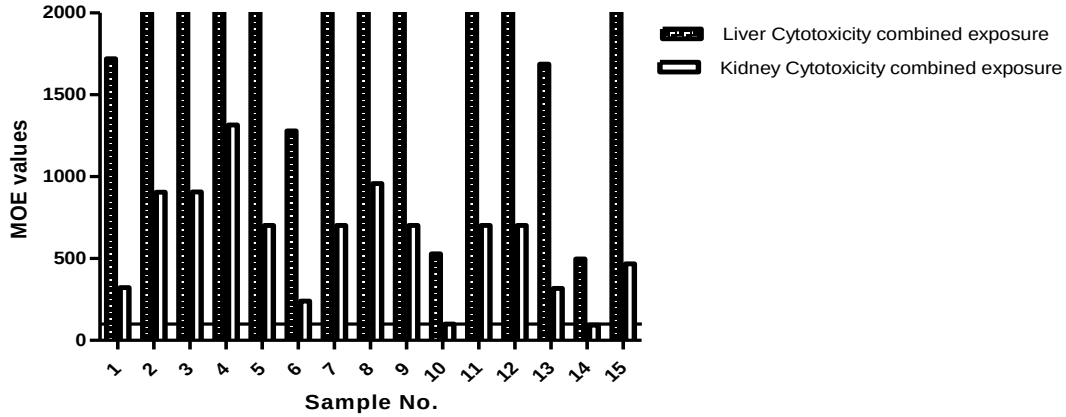

Figure 11: MOE values for liver and kidney cytotoxicity based on the exposure of a) AA-I, b) AA-II and c) Combined exposure of AA-I and AA-II assuming equal potency of toxicity while consuming Indonesian jamu on a daily basis. The line represents the threshold of the MOE of 100. MOE values of the non-detected samples were calculated based on the LoD of 0.9 µM for AA-I and AA-II.

4. DISCUSSION AND CONCLUSION

The aim of the present study was to determine the presence and levels of AAs in Indonesian jamu and to perform an associated risk assessment to see whether there is a priority for risk management. This risk assessment for liver cytotoxicity was carried out by deriving a $BMDL_{10}$ using in vitro data and the PBK modeling approach. The risk assessment for kidney cytotoxicity was carried out based on existing $BMDL_{10}$ values as previously reported by the literature to compare the risk.

Firstly, Indonesian jamu was analyzed for the presence of AAs. In the present study two out of 15 analyzed samples (13.3%) were found to be positive for AAs with an amount of 10.5 and 31.2 µg/g. These findings are in line with other studies which analyzed plant food supplements and other herbal preparations for the presence of AAs. When combining the data of 10 previous studies, a total of 96 out of 397 (24.2%) analyzed samples appeared to contain AAs which ranged from 16 - 1002 µg/g (Cheung et al., 2006), 5 - 162 µg/g (Hsieh et al., 2006), 1.1 - 444 µg/g (Martena et al., 2007), 0.19 - 995 µg/g (Kuo et al., 2010), 0.013 – 3.3 µg/g (Vaclavik et al., 2014), 0.6 – 594.5 µg/g (Abdullah, 2017) or not available/ not specified (Ioset et al., 2003; Koh et al., 2006; Schaneberg & Khan, 2004; Wei et al., 2005). There is a possibility that in the present study an underestimation of the levels of AAs was reported since low percentages of recovery of AA-I and AA-II in powder (0% and 0%), pill (6.7% and 21.8%) and capsule (36.6% and 67.7%) were observed. In most samples of the present study, the chromatogram of the UPLC analysis showed the presence of multiple different compounds in one giant peak, especially at the same retention time as AA-I (6.90 – 6.95 min) and AA-II (6.84 – 6.91 min). The same problem occurred in the spiked samples, which contained an added end concentration of 10 µM (Figure 12). The low percentages of recovery could indicate that a strong matrix effect occurred, because due to complexity in sample constituents, matrix effects are found to be remarkably significant in herbal extracts which adversely effects the outcomes of the analysis (Kuo et al., 2010). Also, due to matrix effects, ingredients could be modified resulting in the toxicity being unchanged, reduced or even increased (Van Den Berg et al., 2011). Different approaches were reported to have been used previously to minimize the matrix effects such as changing and improving sample extraction methods by eliminating undetected matrix interferences and performing the analysis using more efficient chromatographic conditions to separate analytes of interest from other compounds (Matuszewski et al., 2003).

In both positive samples, *Aristolochia debilis* was the suspected botanical. Interestingly, in AA6 both AA-I and AA-II were detected whereas in AA13 only AA-II was detected. This could possibly be due to the differences in matrix effect in the two samples noting that AA6 were pills and AA13 was a liquid sample. The part of the plant and the maturity of the plant used in the samples could also influence the presence of AAs. In a study based on the AA containing *Aristolochia chilensis* it was found that younger leaves contain higher concentrations of AAs than mature leaves. Stems appear to contain even higher concentrations of AAs (Pinto et al., 2009). Since it is unknown which part of the *Aristolochia debilis* was used, how much AAs *Aristolochia debilis* contain and the amount that was used in sample AA6, it is difficult to compare the two samples and speculate further.

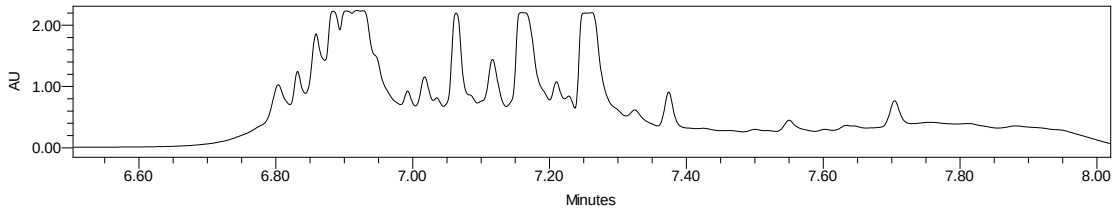

Figure 12: UPLC chromatogram at nm 224 of the methanol extract of sample AA1 spiked with an end concentration of 10 µM AA-I:AA-II mixture. No AAs could be detected from the sample.

The calculated EDI based on the levels of AAs in the positive samples as detected by the UPLC is 1-2 µg/kg bw. This is 0.054 to 0.108 mg per day for a person with an average Indonesian bodyweight. Chinese patients who developed chronic renal failure had ingested an estimated 0.7 to 1.5 mg of aristolochic acids per day intermittently for 1 to 10 years as reported by Grollman et al. (2009). This EDI is a 10-20 fold higher than the EDI calculated for the consumption of the positive Indonesian jamu samples. Further, an intake level of more than 150 mg of AAs ingested via Chinese herbal products were independently associated with an increased risk for urinary tract cancer (Lai et al., 2010). This increased risk will be reached within 4 to 8 years when consuming the Indonesian jamu samples that were found positive for AAs in this present study regularly. Comparison of the intakes and the associated health issues points in the direction that there is a plausible health risk involved with consuming Indonesian jamu regularly.

Because the lack of in vivo tumour data, the in vitro and PBK modeling approach was used to derive the $BMDL_{10}$ which can be used for risk assessment. Big differences were found in the cytotoxicity, both between the HepG2 and HepaRG cells and also between the two different incubations of the same cell line. The fraction unbound of AA-I in vitro was calculated to be 0.0864 so the difference in cytotoxicity within the same cell line using different incubations should be about a 12-fold. Larger differences were observed which are difficult to explain since besides the FCS, all factors were the same. When comparing the different cell lines, it is clearly shown that HepaRG cells were more sensitive to the cytotoxic characteristics of AA-I as compared to HepG2 cells. This can be explained by the fact that HepaRG cells have higher drug metabolizing enzyme activities as compared to HepG2 cells (Yokoyama et al., 2018). These high metabolizing characteristics of HepaRG cells contribute to a higher reductive activation rate of AA-I which leads to the higher cytotoxicity. Further, in vitro data from the literature showed similar cytotoxicity levels in HepG2 cells upon synthesized AA-I exposure as compared to the exposed HepG2 cells from the present study (Nitzsche et al., 2013). Also in the human hepatic cell lines Bel-7402, Hl-7702 and L-02 cytotoxicity results based on synthesized AA-I were within the range of the cytotoxicity found in this present study (Liu et al., 2015; Yuan et al., 2009; L. Zhang et al., 2007). When the HepG2 cells were exposed to mother tincture of *Aristolochia europaeum* and *Aristolochia clematitis*, cytotoxic effects already occurred at way lower exposure levels but this may be due to other unknown toxicants present in the mother tincture (Nitzsche et al., 2013). For the HepaRG cell line, no literature data is available to compare the outcomes. In primary human renal cells (incubated with FCS) cytotoxic effects were observed at way lower levels than in the present study with an IC_{10} of 0.3-1.5 µM and also in the pig renal cell line LLC-PK1, IC_{10} values in between 1.4-1.6 µM were found (Abdullah, 2017; Huljic

et al., 2008). The LCC-PK1 pig kidney cell line was included in this comparison since it is a valuable cell line to assess the kidney toxicity of AA-I for humans in vitro. This is because the genetic proximity of humans and pigs, the anatomical and physiological similarities of the kidneys and because AA-I toxicity directly focuses on the proximal tubular tissue (Huljic et al., 2008). Furthermore it is observed that cytotoxic effects in the liver tissue occur upon an exposure level of >3 µM AA-I in HepG2 cells and even of >10 µM AA-I in HepaRG cells whereas in the primary human renal cells and the LCC-PK1 cells a cytotoxic effect already occurs at a concentration level in the kidney tissue of 0.1 - 0.5 µM. This comparison shows a higher cytotoxic effect of AA-I in kidney tissue as compared to liver tissue in vitro.

Data on DNA-adduct formation in vitro was gathered by exposing HepG2 cells to a range of levels of AA-I where dA-AA-I appeared to be the major DNA-adduct formed. At exposure levels below 10 µM, no DNA-adduct formation was observed which was in line with the findings of the cytotoxicity assay of the present study where also at an exposure level of 10 µM and higher adverse effects were observed. This indicates that in between a concentration level of >3 to 10 µM in the human liver tissue in vitro the first visible adverse effects occur. Similar DNA-adduct formation between studies was found for exposure of AA-I to hepG2 cells as reported by Nitzsche et al. (2013). It is however unclear whether the cytotoxic and DNA-forming effects also occurred above a certain threshold in between >3 to 10 µM since the study started with an exposure level of AA-I of > 10 µM. In the pig kidney cell line LCC-PK1, DNA-adducts already started to form at exposure levels between 0.5 – 2 µM and in higher levels as compared to the HepG2 cells (Abdullah, 2017; Romanov et al., 2012). The comparison of DNA-adduct formation in the liver and kidney points to a clear direction of the kidney being the target organ for carcinogenicity which has been studied thoroughly (Bieler et al., 1997; Schmeiser et al., 1996; Schmeiser et al., 2014). Still, the results also indicate that there is a risk of tumour development in the liver upon AA exposure. This is confirmed by the findings in an AAN patient post-mortem, where a poorly differentiated carcinoma was found in the liver (Arlt et al., 2004).

All parameters used in the PBK model were described previously by Abdullah (2017). The absorption rate constant was assumed based on rat studies and the biliary excretion rate constant and the urine excretion rate constant were scaled via allometric scaling (Ren et al., 2014; Su et al., 2004). These parameters could, even though the assumption and the allometric scaling were based on literature (Lin, 1998; Sharma & McNeill, 2009; Yan et al., 2012), give uncertain results since it is not based on human in vivo studies and thus not validated in that sense. Especially since the absorption rate constant and the biliary excretion rate constant were the most sensitive parameters of the PBK model, they may influence the C_{max} of AA-I in the liver tissue upon exposure significantly. Moreover, no in vivo kinetic data of AA-I in humans was available which means the prediction of the human PBK model cannot be validated. Because of ethical endpoints, this will not become a recommendation for further research. However, the parameters used by Abdullah (2017) for predicting the C_{max} in rats was validated by in vivo kinetic data. Since the parameters from rat and humans were obtained via the same literature (physiological and physiochemical) and by performing the same type of in vitro assay (kinetic), it is reasonable to assume that the physiological, physiochemical and kinetic parameters used in the PBK model were valid.

The goal of using the PBK modeling reverse dosimetry approach in the present study was to translate the concentration-response curves to dose-response curves. The $BMDL_{10}$ values that were calculated from the corrected data became really high, except the $BMDL_{10}$ value based on the HepaRG cells incubated without FCS in vitro. The high $BMDL_{10}$ values for the acute liver tissue injury can be explained by the low unbound fraction of AA-I of 0.56% in vivo which means that high amounts of AA-I should be ingested to get the C_{max} and the corresponding cytotoxicity and DNA-adduct formation in the liver tissue as tested by the in vitro assays. The unbound fraction calculated is in line with a study from Li et al. (2015) who reported data that resulted in even higher fractions unbound of 0.0123 in vitro and 0.0007 in vivo. The low fractions unbound confirm the high affinity of AA-I to bind to proteins. It is important to note that the high $BMDL_{10}$ values for acute liver toxicity do not necessarily mean a low risk of AA-I in the human body. Because of the high binding of AAs to serum albumins, AAs can be stored in the body as protein bound complex for a long time. These complexes can gradually release AAs in the body which leads to a chronic exposure to AA-I in human tissues and exhibits its toxicological effects (Li et al., 2015).

Another important note is that when the cells that were incubated without FCS were corrected for the fraction unbound, the dose-response curves should have been similar to the ones incubated with FCS (results section, Figure 9). This is however not the case which indicates that different types of incubations will lead to different cytotoxicity data even after correction for protein binding. Furthermore, contradictive results were found after the correction for protein binding meaning that the lowest and highest $BMDL_{10}$ found were both based on the incubation of the cell lines without FCS. Therefore it also doesn't indicate that the fraction unbound factors give higher or lower cytotoxicity data after correction, making the results of the present study difficult to interpret.

Then, the outcomes of the $BMDL_{10}$ as obtained by the predicted dose-response data from the PBK model could not be compared to human in vivo data since these are lacking. This is an important problem for validating the calculated $BMDL_{10}$ since it is completely unclear whether the predictions are within the normal range of effects that will occur in the human body. The $BMDL_{10}$ values for the kidney as previously predicted by the same PBK model for cytotoxicity were 0.5-1.1 mg/kg bw (Huljic et al., 2008) and 1.0 -1.2 mg/kg bw (Abdullah, 2017). Similarly to the comparison based on the in vitro assays, the kidney seems to be at a greater risk of cytotoxicity upon AA-I exposure as compared to the liver based on the $BMDL_{10}$ values. The $BMDL_{10}$ for the DNA-adduct formation predicted by the same PBK model was reported to be 0.04-0.11 mg/kg bw by Abdullah (2017). The difference between those values and the values of the present study (90.5 mg/kg bw) were exceptionally large. This is partly due to the use of a different fraction unbound of 0.22 in the study of Abdullah (2017), but when applying the same factor of the fraction unbound the differences remain large. These differences can, as already stated before, be explained by the fact that in the liver the first formation of DNA-adducts was observed at an exposure level of 10 µM whereas in the kidney already after an exposure of 0.5 µM high amounts of DNA-adducts were found. This clearly shows a way higher carcinogenicity in the kidney as compared to the liver. The reason for the large difference is unknown and the preference of AA-I to target the kidney remains unclear.

To carry out the risk assessment of Indonesian jamu for liver cytotoxicity, the $BMDL_{10}$ of 2.66 mg/kg bw was used to determine the MOE values. For the same risk assessment for kidney cytotoxicity, the lowest $BMDL_{10}$ value of 0.5 mg/kg bw was used based on the data of Huljic et al. (2008). The risk assessments show that the MOE values for kidney cytotoxicity are a 5-fold lower as compared to the liver cytotoxicity, which confirms the current state of the art conform the kidney being the target organ for AAs to induce injury (Arlt et al., 2001; Cosyns et al., 1994; Gillerot et al., 2001; Joëlle L Nortier et al., 2003; Schmeiser et al., 1996; J.-L. Vanherweghem et al., 1993; L. J. Vanherweghem, 1998). Still, most MOE values found in this present study indicate no priority for risk management based on both liver and kidney cytotoxicity. Only the combined exposure of AAs in AA10 and AA14 gave an indication for the priority for risk management. However, in both samples AAs were not detected by the UPLC analysis and thus this indication is based on the calculation of the LoD which makes it weakly underpinned to base the priority of risk management on this data. In contrast, based on the risk assessment as carried out by Abdullah (2017) for carcinogenicity data, it was found that AAs in plant food supplements and other herbal products were a priority for risk management.

The present study gives a nice first overview about the risk of AAs that are present in Indonesian jamu. For further research, it is recommended to take a deeper look into the possible matrix effects of Indonesian jamu and their influence on the detected amount of AAs by UPLC analysis. If possible, also the part and maturity of the plant used in Indonesian jamu should be taking into account to determine the risk more specifically. Then, the translation of the concentration-response curves to the predicted dose-response curves resulted in big differences in $BMDL_{10}$ values after correcting the concentration-response data for the fraction unbound. This is a relevant topic for further research since now different incubation types give different $BMDL_{10}$ values whereas after the correction the results should be similar. To solve this, it might be useful to experiment with different exposure methods to see which methods give reliable results when cells get incubated with and without FCS and corrected for the unbound fraction hereafter. Furthermore, the outcome of the PBK model gave a nice indication of what amount of AA will reach the liver tissue upon a certain oral dose. These parameters were validated previously by Abdullah (2017) based on well thought assumptions and allometric scaling according to literature. Since it is unethical to perform human studies, this is probably about the most specific that the parameters will get and no further research is recommended for this part. Based on the MOE values, it seems no priority that risk management will be carried out to protect human health for kidney and liver toxicity upon AA exposure since most MOE values were above the threshold of 100. Only the combined exposure of AAs in AA10 and AA14 had lower MOE values of 99.5 and 93.4 respectively and these were both samples in which AAs were not detected in the UPLC analysis.

It is concluded that AAs were present in 13.3% of the analyzed Indonesian jamu samples but that these samples don't pose a health concern for both kidney and liver cytotoxicity when consuming Indonesian jamu regularly. For the samples in which no AAs were detected but was assumed that the amount of AAs present was equal to the LoD, a priority for risk management was found in 15.4% of the undetected samples. Lastly, the kidney seems to be the target organ for both the cytotoxicity and DNA-adduct formation as compared to the liver which is in line with the current state of the art that AAs are

nephrotoxic and carcinogenic. It is thus preferred that the focus of future research will remain on the kidney.

5. REFERENCES

Abdullah, R. (2017). *Integrated strategy for the assessment of kidney toxicity.* Wageningen University.

Afdhal, A. F., & Welsch, R. L. (1988). The rise of the modern jamu industry in Indonesia: a preliminary overview *The Context of Medicines in Developing Countries* (pp. 149-172): Springer.

Afendi, F. M., Okada, T., Yamazaki, M., Hirai-Morita, A., Nakamura, Y., Nakamura, K., . . . Darusman, L. K. (2011). KNApSAcK family databases: integrated metabolite–plant species databases for multifaceted plant research. *Plant and Cell Physiology, 53*(2), e1-e1.

Ali, N., Hashim, N., Saad, B., Safan, K., Nakajima, M., & Yoshizawa, T. (2005). Evaluation of a method to determine the natural occurrence of aflatoxins in commercial traditional herbal medicines from Malaysia and Indonesia. *Food and Chemical Toxicology, 43*(12), 1763-1772.

Amersham Biosciences, A. (2004). Unicorn 5.0 User Reference Manual. 406-407. doi: https://btiscience.org/wp-content/uploads/2014/04/UNICORN_User_Manual.pdf

Anderson, L., & Vlietinck, A. (2000). Position paper on the risks associated with the use of herbal products containing Aristolochia species *Working Party on Herbal Medicinal Products, the European Agency for the Evaluation of Medicinal Products, EMEA, HMPPWP 23/00, September 2000* (pp. 1-9).

Arlt, V. M., Alunni-Perret, V., Quatrehomme, G., Ohayon, P., Albano, L., Gaïd, H., . . . Wiessler, M. (2004). Aristolochic acid (AA)-DNA adduct as marker of AA exposure and risk factor for AA nephropathy-associated cancer. *International journal of cancer, 111*(6), 977-980.

Arlt, V. M., Schmeiser, H. H., & Pfeifer, G. P. (2001). Sequence-specific detection of aristolochic acid–DNA adducts in the human p53 gene by terminal transferase-dependent PCR. *Carcinogenesis, 22*(1), 133-140.

Arlt, V. M., Stiborova, M., & Schmeiser, H. H. (2002). Aristolochic acid as a probable human cancer hazard in herbal remedies: a review. *Mutagenesis, 17*(4), 265-277.

Barlow, S., Renwick, A., Kleiner, J., Bridges, J., Busk, L., Dybing, E., . . . Knaap, A. (2006). Risk assessment of substances that are both genotoxic and carcinogenic: report of an International Conference organized by EFSA and WHO with support of ILSI Europe. *Food and Chemical Toxicology, 44*(10), 1636-1650.

Beers, S.-J. (2012). *Jamu: the ancient Indonesian art of herbal healing*: Tuttle Publishing.

Benford, D., Bolger, P. M., Carthew, P., Coulet, M., DiNovi, M., Leblanc, J.-C., . . . Smith, B. (2010). Application of the margin of exposure (MOE) approach to substances in food that are genotoxic and carcinogenic. *Food and Chemical Toxicology, 48*, S2-S24.

Berezhkovskiy, L. M. (2004). Volume of distribution at steady state for a linear pharmacokinetic system with peripheral elimination. *Journal of pharmaceutical sciences, 93*(6), 1628-1640.

Bieler, C., Stiborova, M., Wiessler, M., Cosyns, J.-P., Van Ypersele de Strihou, C., & Schmeiser, H. (1997). 32P-post-labelling analysis of DNA adducts formed by aristolochic acid in tissues from patients with Chinese herbs nephropathy. *Carcinogenesis, 18*(5), 1063-1067.

Brown, R. P., Delp, M. D., Lindstedt, S. L., Rhomberg, L. R., & Beliles, R. P. (1997). Physiological parameter values for physiologically based pharmacokinetic models. *Toxicology and industrial health, 13*(4), 407-484.

Chen, L., Ning, J., Louisse, J., Wesseling, S., & Rietjens, I. M. (2018). Use of physiologically based kinetic modelling-facilitated reverse dosimetry to convert in vitro cytotoxicity data to predicted in vivo liver toxicity of lasiocarpine and riddelliine in rat. *Food and Chemical Toxicology, 116*, 216-226.

Chen, M., Gong, L., Qi, X., Xing, G., Luan, Y., Wu, Y., . . . Xue, X. (2011). Inhibition of renal NQO1 activity by dicoumarol suppresses nitroreduction of aristolochic acid I and attenuates its nephrotoxicity. *Toxicological Sciences, 122*(2), 288-296.

Cheung, T. P., Xue, C., Leung, K., Chan, K., & Li, C. G. (2006). Aristolochic acids detected in some raw Chinese medicinal herbs and manufactured herbal products–a consequence of inappropriate nomenclature and imprecise labelling? *Clinical Toxicology, 44*(4), 371-378.

Clewell, R. A., & Clewell III, H. J. (2008). Development and specification of physiologically based pharmacokinetic models for use in risk assessment. *Regulatory Toxicology and Pharmacology, 50*(1), 129-143.

Cosyns, J.-P., Jadoul, M., Squifflet, J.-P., Van Cangh, P.-J., & de Strihou, C. v. Y. (1994). Urothelial malignancy in nephropathy due to Chinese herbs. *The Lancet, 344*(8916), 188.

Debelle, F. D., Vanherweghem, J.-L., & Nortier, J. L. (2008). Aristolochic acid nephropathy: a worldwide problem. *Kidney international, 74*(2), 158-169.

Dong, H., Suzuki, N., Torres, M. C., Bonala, R. R., Johnson, F., Grollman, A. P., & Shibutani, S. (2006). QUANTITATIVE DETERMINATION OF ARISTOLOCHIC ACID-DERIVED DNA ADDUCTS IN RATS USING ³²P-POSTLABELING/POLYACRYLAMIDE GEL ELECTROPHORESIS ANALYSIS. *Drug metabolism and disposition, 34*(7), 1122-1127. doi: 10.1124/dmd.105.008706

EFSA. (2005). Opinion of the Scientific Committee on a request from EFSA related to A Harmonised Approach for Risk Assessment of Substances Which are both Genotoxic and Carcinogenic. *EFSA Journal, 3*(10), 282. doi: doi:10.2903/j.efsa.2005.282
Elfahmi, Woerdenbag, H. J., & Kayser, O. (2014). Jamu: Indonesian traditional herbal medicine towards rational phytopharmacological use. *Journal of Herbal Medicine, 4*(2), 51-73. doi: https://doi.org/10.1016/j.hermed.2014.01.002
EMEA. (1997). Commitee for veterinary medicinal products aristolochia summary report. *The European Agency for the Evaluation of Medicinal Products*(EMEA/MRL/271/97-FINAL).
FAO/WHO. (2005). *Summary and conclusions of the sixty-fourth meeting of the Joint FAO/WHO Expert Committee on Food Additives (JECFA)*. Rome, Italy: Retrieved from http://www.fao.org/3/a-at877e.pdf.
FAO/WHO. (2014). *Guidelines for Simple Evaluation of Dietary Exposure to Food Additives* (CAC/GL 3-1989). Food and Agriculture Organization of the United Nations, World Health Organization
FAO/WHO/UNU, J. (1981). *BODY WEIGHTS AND HEIGHTS BY COUNTRIES. Joint FAO/WHO/UNU Expert Consultation on Energy and Protein Requirements.* . Rome, 5 to 17 October 1981: Food and Agriculture Organization of the United Nations, World Health Organization, The United Nations University Retrieved from http://www.fao.org/docrep/meeting/004/M2846E/M2846E00.htm.
FDA. (2001). *Aristolochic Acid: Listing of Botanical Ingredients of Concern*. Retrieved from http://wayback.archive-it.org/7993/20171115154511/https://www.fda.gov/Food/RecallsOutbreaksEmergencies/SafetyAlertsAdvisories/ucm095283.htm.
Gerlowski, L. E., & Jain, R. K. (1983). Physiologically based pharmacokinetic modeling: principles and applications. *Journal of pharmaceutical sciences, 72*(10), 1103-1127.
Gillerot, G., Jadoul, M., Arlt, V. M., de Strihou, C. v. Y., Schmeiser, H. H., But, P. P., . . . Cosyns, J.-P. (2001). Aristolochic acid nephropathy in a Chinese patient: time to abandon the term “Chinese herbs nephropathy”? *American Journal of Kidney Diseases, 38*(5), E26.
Grollman, A. P., Scarborough, J., & Jelaković, B. (2009). Aristolochic acid nephropathy: an environmental and iatrogenic disease. *Advances in molecular toxicology, 3*, 211-227.
Grollman, A. P., Shibutani, S., Moriya, M., Miller, F., Wu, L., Moll, U., . . . Medverec, Z. (2007). Aristolochic acid and the etiology of endemic (Balkan) nephropathy. *Proceedings of the National Academy of Sciences, 104*(29), 12129-12134.
Guengerich, F. P. (2000). Metabolism of chemical carcinogens. *Carcinogenesis, 21*(3), 345-351.
Gülden, M., & Seibert, H. (2003). In vitro–in vivo extrapolation: estimation of human serum concentrations of chemicals equivalent to cytotoxic concentrations in vitro. *Toxicology, 189*(3), 211-222.
Han, S.-y., Qiao, J.-q., Zhang, Y.-y., Lian, H.-z., & Ge, X. (2012). Determination of n-octanol/water partition coefficients of weak ionizable solutes by RP-HPLC with neutral model compounds. *Talanta, 97*, 355-361.
Heinrich, M., Chan, J., Wanke, S., Neinhuis, C., & Simmonds, M. S. (2009). Local uses of Aristolochia species and content of nephrotoxic aristolochic acid 1 and 2--a global assessment based on bibliographic sources. *J Ethnopharmacol, 125*(1), 108-144. doi: 10.1016/j.jep.2009.05.028
Hong, Y.-T., Fu, L.-S., Chung, L.-H., Hung, S.-C., Huang, Y.-T., & Chi, C.-S. (2006). Fanconi’s syndrome, interstitial fibrosis and renal failure by aristolochic acid in Chinese herbs. *Pediatric Nephrology, 21*(4), 577-579.
Hranjec, T., Kovač, A., Kos, J., Mao, W., Chen, J. J., Grollman, A. P., & Jelaković, B. (2005). Endemic nephropathy: the case for chronic poisoning by aristolochia. *Croatian medical journal, 46*(1).
Hsieh, S.-C., Huang, M.-F., Lin, B.-S., & Chang, H.-T. (2006). Determination of aristolochic acid in Chinese herbal medicine by capillary electrophoresis with laser-induced fluorescence detection. *Journal of Chromatography A, 1105*(1-2), 127-134.
Huljic, S., Bruske, E. I., Pfitzenmaier, N., O’Brien, E., & Dietrich, D. R. (2008). Species-specific toxicity of aristolochic acid (AA) in vitro. *Toxicology in vitro, 22*(5), 1213-1221.
IARC, W. G. o. t. E. o. C. R. t. H. (2012). Pharmaceuticals. Volume 100 A. A review of human carcinogens. *IARC monographs on the evaluation of carcinogenic risks to humans, 100*(PT A), 1.
IARC, W. G. o. t. E. o. C. R. t. H., Organization, W. H., & Cancer, I. A. f. R. o. (2002). *Some traditional herbal medicines, some mycotoxins, naphthalene and styrene*: World Health Organization.
ICH, H. T. G. (2005). *Validation of analytical procedures: text and methodology Q2 (R1).* Paper presented at the International Conference on Harmonization, Geneva, Switzerland.
Ioset, J.-R., Raoelison, G., & Hostettmann, K. (2003). Detection of aristolochic acid in Chinese phytomedicines and dietary supplements used as slimming regimens. *Food and Chemical Toxicology, 41*(1), 29-36.
Jadot, I., Declèves, A.-E., Nortier, J., & Caron, N. (2017). An Integrated View of Aristolochic Acid Nephropathy: Update of the Literature. *International Journal of Molecular Sciences, 18*(2), 297.
Jelaković, B., Nikolić, J., Radovanović, Z., Nortier, J., Cosyns, J.-P., Grollman, A. P., . . . Čavaljuga, S. (2013). Consensus statement on screening, diagnosis, classification and treatment of endemic (Balkan) nephropathy. *Nephrology Dialysis Transplantation, 29*(11), 2020-2027.
Jennen, D. G., Magkoufopoulou, C., Ketelslegers, H. B., van Herwijnen, M. H., Kleinjans, J. C., & van Delft, J. H. (2010). Comparison of HepG2 and HepaRG by whole-genome gene expression analysis for the purpose of chemical hazard identification. *Toxicological Sciences, 115*(1), 66-79.
Kanebratt, K. P., & Andersson, T. B. (2008). Evaluation of HepaRG cells as an in vitro model for human drug metabolism studies. *Drug metabolism and disposition, 36*(7), 1444-1452.

Kevekordes, S., Spielberger, J., Burghaus, C., Birkenkamp, P., Zietz, B., Paufler, P., . . . Dunkelberg, H. (2001). Micronucleus formation in human lymphocytes and in the metabolically competent human hepatoma cell line Hep-G2: results with 15 naturally occurring substances. *Anticancer research, 21*(1A), 461-469.
Knasmüller, S., Parzefall, W., Sanyal, R., Ecker, S., Schwab, C., Uhl, M., . . . Langer, T. (1998). Use of metabolically competent human hepatoma cells for the detection of mutagens and antimutagens. *Mutation Research/Fundamental and Molecular Mechanisms of Mutagenesis, 402*(1-2), 185-202.
Koh, H., Wang, H., Zhou, S., Chan, E., & Woo, S. (2006). Detection of aristolochic acid I, tetrandrine and fangchinoline in medicinal plants by high performance liquid chromatography and liquid chromatography/mass spectrometry. *Journal of pharmaceutical and biomedical analysis, 40*(3), 653-661.
Krewski, D., Withey, J. R., Ku, L.-f., & Andersen, M. E. (1994). Applications of physiologic pharmacokinetic modeling in carcinogenic risk assessment. *Environmental Health Perspectives, 102*(suppl 11), 37-50.
Krishnan, K., & Andersen, M. (2001). Principles and methods of toxicology: Taylor & Francis, 4ºed., London.
Kumar, V., Poonam, Prasad, A. K., & Parmar, V. S. (2003). Naturally occurring aristolactams, aristolochic acids and dioxoaporphines and their biological activities. *Nat Prod Rep, 20*(6), 565-583.
Kuo, C.-H., Lee, C.-W., Lin, S.-C., Tsai, I.-L., Lee, S.-S., Tseng, Y. J., . . . Wei-Chu, L. (2010). Rapid determination of aristolochic acids I and II in herbal products and biological samples by ultra-high-pressure liquid chromatography–tandem mass spectrometry. *Talanta, 80*(5), 1672-1680.
Lai, M.-N., Wang, S.-M., Chen, P.-C., Chen, Y.-Y., & Wang, J.-D. (2010). Population-based case–control study of Chinese herbal products containing aristolochic acid and urinary tract cancer risk. *Journal of the National Cancer Institute, 102*(3), 179-186.
Li, W., Hu, Q., & Chan, W. (2015). Mass Spectrometric and Spectrofluorometric Studies of the Interaction of Aristolochic Acids with Proteins. *Scientific reports, 5*, 15192.
Lin, J. H. (1998). Applications and limitations of interspecies scaling and in vitro extrapolation in pharmacokinetics. *Drug metabolism and disposition, 26*(12), 1202-1212.
Liu, X., Liu, Y., Cheng, M., & Xiao, H. (2015). Metabolomic responses of human hepatocytes to emodin, aristolochic acid, and triptolide: chemicals purified from traditional Chinese medicines. *Journal of biochemical and molecular toxicology, 29*(11), 533-543.
Lord, G. M., Hollstein, M., Arlt, V. M., Roufosse, C., Pusey, C. D., Cook, T., & Schmeiser, H. H. (2004). DNA adducts and p53 mutations in a patient with aristolochic acid-associated nephropathy. *American Journal of Kidney Diseases, 43*(4), e18. 11-e18. 17.
Louisse, J., de Jong, E., van de Sandt, J. J., Blaauboer, B. J., Woutersen, R. A., Piersma, A. H., . . . Verwei, M. (2010). The use of in vitro toxicity data and physiologically based kinetic modeling to predict dose-response curves for in vivo developmental toxicity of glycol ethers in rat and man. *Toxicological Sciences, 118*(2), 470-484.
Martena, M. J., van der Wielen, J. C. A., van de Laak, L. F. J., Konings, E. J. M., de Groot, H. N., & Rietjens, I. M. C. M. (2007). Enforcement of the ban on aristolochic acids in Chinese traditional herbal preparations on the Dutch market. *Analytical and Bioanalytical Chemistry, 389*(1), 263-275. doi: 10.1007/s00216-007-1310-3
Martinek, V., Kubickova, B., Arlt, V. M., Frei, E., Schmeiser, H. H., Hudecek, J., & Stiborova, M. (2011). Comparison of activation of aristolochic acid I and II with NADPH: quinone oxidoreductase, sulphotransferases and N-acetyltranferases. *Neuro endocrinology letters, 32*, 57-70.
Matuszewski, B., Constanzer, M., & Chavez-Eng, C. (2003). Strategies for the assessment of matrix effect in quantitative bioanalytical methods based on HPLC− MS/MS. *Analytical chemistry, 75*(13), 3019-3030.
Mei, N., Arlt, V. M., Phillips, D. H., Heflich, R. H., & Chen, T. (2006). DNA adduct formation and mutation induction by aristolochic acid in rat kidney and liver. *Mutation Research/Fundamental and Molecular Mechanisms of Mutagenesis, 602*(1), 83-91.
Milichovský, J., Bárta, F., Schmeiser, H. H., Arlt, V. M., Frei, E., Stiborová, M., & Martínek, V. (2016). Active site mutations as a suitable tool contributing to explain a mechanism of aristolochic acid I nitroreduction by cytochromes P450 1A1, 1A2 and 1B1. *International Journal of Molecular Sciences, 17*(2), 213.
MoH. (2007). *National policy on Traditional Medicine, (RI MoH ed)*. Jakarta: Retrieved from http://www.searo.who.int/entity/medicines/topics/national_policy_on_traditional_medicines_ministry_of_health.pdf.
MoH. (2013). *Riset Kesehatan Dasar Riskesdas 2013*. Jakarta: Retrieved from http://www.depkes.go.id/resources/download/general/Hasil%20Riskesdas%202013.pdf
NADFC. (2015). *Laporan Tahunan Badan POM 2015. The national agency for drug and food control (NADFC) of Indonesia.*: Retrieved from http://www.pom.go.id/ppid/rar/2016/laptah2014.pdf
NADFC. (2017). *Badan Pendawas Obat Dan Makanan Laporan Tahunan 2016. The national agency for drug and food control (NADFC) of Indonesia.* . Retrieved from http://www.pom.go.id/new/admin/dat/20171127/laptah2016.pdf
Nitzsche, D., Melzig, M. F., & Arlt, V. M. (2013). Evaluation of the cytotoxicity and genotoxicity of aristolochic acid I–A component of Aristolochiaceae plant extracts used in homeopathy. *Environmental toxicology and pharmacology, 35*(2), 325-334.
Nortier, J. L., Martinez, M.-C. M., Schmeiser, H. H., Arlt, V. M., Bieler, C. A., Petein, M., . . . Vereerstraeten, P. (2000). Urothelial carcinoma associated with the use of a Chinese herb (Aristolochia fangchi). *New England Journal of Medicine, 342*(23), 1686-1692.
Nortier, J. L., Schmeiser, H. H., Martinez, M. C. M., Arlt, V. M., Vervaet, C., Garbar, C. H., . . . Vanherweghem, J. L. (2003). Invasive urothelial carcinoma after exposure to Chinese herbal medicine containing

aristolochic acid may occur without severe renal failure. *Nephrology Dialysis Transplantation, 18*(2), 426-428.
NTP. (2016). *Report on Carcinogens, Fourteenth Edition.* NC: U.S.: National Toxicology Program: Research Triangle Park Retrieved from Https://ntp.niehs.nih.gov/ntp/roc/content/profiles/aristolochicacids.pdf.
Pfau, W., Schmeiser, H. H., & Wiessler, M. (1990). Aristolochic acid binds covalently to the exocyclic amino group of purine nucleotides in DNA. *Carcinogenesis, 11*(2), 313-319.
Pinto, C. F., Troncoso, A. J., Urzúa, A., & Niemeyer, H. M. (2009). Aristolochic acids affect the feeding behaviour and development of Battus polydamas archidamas larvae (Lepidoptera: Papilionidae: Troidini). *European Journal of Entomology, 106*(3), 357.
Punt, A., Freidig, A. P., Delatour, T., Scholz, G., Boersma, M. G., Schilter, B., . . . Rietjens, I. M. (2008). A physiologically based biokinetic (PBBK) model for estragole bioactivation and detoxification in rat. *Toxicology and applied pharmacology, 231*(2), 248-259.
Ren, G., Huang, Q., Wu, J., Yuan, J., Yang, G., Yan, Z., & Yao, S. (2014). Cloud point extraction–HPLC method for the determination and pharmacokinetic study of aristolochic acids in rat plasma after oral administration of Aristolochiae Fructus. *Journal of Chromatography B, 953*, 73-79.
Rietjens, I. M., Louisse, J., & Punt, A. (2011). Tutorial on physiologically based kinetic modeling in molecular nutrition and food research. *Molecular nutrition & food research, 55*(6), 941-956.
Rietjens, I. M., Martena, M. J., Boersma, M. G., Spiegelenberg, W., & Alink, G. M. (2005). Molecular mechanisms of toxicity of important food-borne phytotoxins. *Molecular nutrition & food research, 49*(2), 131-158.
Romanov, V., Sidorenko, V., Rosenquist, T. A., Whyard, T., & Grollman, A. P. (2012). A fluorescence-based analysis of aristolochic acid-derived DNA adducts. *Analytical biochemistry, 427*(1), 49-51.
Rosenquist, T. A., & Grollman, A. P. (2016). Mutational signature of aristolochic acid: Clue to the recognition of a global disease. *DNA repair, 44*, 205-211. doi: https://doi.org/10.1016/j.dnarep.2016.05.027
Schaneberg, B., & Khan, I. (2004). Analysis of products suspected of containing Aristolochia or Asarum species. *J Ethnopharmacol, 94*(2-3), 245-249.
Schmeiser, H. H., Bieler, C. A., Wiessler, M., de Strihou, C. v. Y., & Cosyns, J.-P. (1996). Detection of DNA adducts formed by aristolochic acid in renal tissue from patients with Chinese herbs nephropathy. *Cancer Research, 56*(9), 2025-2028.
Schmeiser, H. H., Nortier, J. L., Singh, R., Gamboa da Costa, G., Sennesael, J., Cassuto-Viguier, E., . . . Phillips, D. H. (2014). Exceptionally long-term persistence of DNA adducts formed by carcinogenic aristolochic acid I in renal tissue from patients with aristolochic acid nephropathy. *International journal of cancer, 135*(2), 502-507.
Scientific, T. (2013). Assessment of nucleic acid purity. *T042-Technical Bulletin Nano Drop Spectrophotometers, nanodrop. com/Library/TO42-NanoDrop-Spectrophotometer-Nucleic-Acid-Purity-Ratios. pdf. Accessed 20th November*.
Sharma, V., & McNeill, J. H. (2009). To scale or not to scale: the principles of dose extrapolation. *British journal of pharmacology, 157*(6), 907-921.
Shibutani, S., Dong, H., Suzuki, N., Ueda, S., Miller, F., & Grollman, A. P. (2007). Selective toxicity of aristolochic acids I and II. *Drug metabolism and disposition*.
Stiborová, M., Arlt, V. M., & Schmeiser, H. H. (2017). DNA adducts formed by aristolochic acid are unique biomarkers of exposure and explain the initiation phase of upper urothelial cancer. *International Journal of Molecular Sciences, 18*(10), 2144.
Stiborová, M., Frei, E., Arlt, V. M., & Schmeiser, H. H. (2008). Metabolic activation of carcinogenic aristolochic acid, a risk factor for Balkan endemic nephropathy. *Mutation Research/Reviews in Mutation Research, 658*(1-2), 55-67.
Stiborová, M., Frei, E., & Schmeiser, H. (2008). Biotransformation enzymes in development of renal injury and urothelial cancer caused by aristolochic acid. *Kidney international, 73*(11), 1209-1211.
Su, T., Qu, L., Zhang, C., Cai, S., & Li, X. (2004). Studies on pharmacodynamic characteristics of aristolochic acid I in rats. *Zhongguo Zhong yao za zhi= Zhongguo zhongyao zazhi= China journal of Chinese materia medica, 29*(7), 676-681.
Suparmi, S., Widiastuti, D., Wesseling, S., & Rietjens, I. M. C. M. (2018). Natural occurrence of genotoxic and carcinogenic alkenylbenzenes in Indonesian jamu and evaluation of consumer risks. *Food and Chemical Toxicology, 118*, 53-67. doi: https://doi.org/10.1016/j.fct.2018.04.059
Tian-Shung, W., Amooru, D., Chung-Ren, S., & Ping-Chung, K. (2005). Chemical constituents and pharmacology of Aristolochi species *Studies in Natural Products Chemistry* (Vol. 32, pp. 855-1018): Elsevier.
Vaclavik, L., Krynitsky, A. J., & Rader, J. I. (2014). Quantification of aristolochic acids I and II in herbal dietary supplements by ultra-high-performance liquid chromatography–multistage fragmentation mass spectrometry. *Food Additives & Contaminants: Part A, 31*(5), 784-791.
Van Den Berg, S. J., Restani, P., Boersma, M. G., Delmulle, L., & Rietjens, I. M. (2011). Levels of genotoxic and carcinogenic ingredients in plant food supplements and associated risk assessment.
Vanherweghem, J.-L., Tielemans, C., Abramowicz, D., Depierreux, M., Vanhaelen-Fastre, R., Vanhaelen, M., . . . Verbeelen, D. (1993). Rapidly progressive interstitial renal fibrosis in young women: association with slimming regimen including Chinese herbs. *The Lancet, 341*(8842), 387-391.
Vanherweghem, L. J. (1998). Misuse of herbal remedies: the case of an outbreak of terminal renal failure in Belgium (Chinese herbs nephropathy). *J Altern Complement Med, 4*(1), 9-13. doi: 10.1089/acm.1998.4.1-9

Wei, F., Cheng, X. L., Ma, L. Y., Jin, W. T., Schaneberg, B. T., Khan, I. A., & Lin, R. C. (2005). Analysis of aristolochic acids and analogues in medicinal plants and their commercial products by HPLC-PAD-ESI/MS. *Phytochemical Analysis: An International Journal of Plant Chemical and Biochemical Techniques, 16*(3), 222-230.

Woerdenbag, H. J., & Kayser, O. (2014). Jamu: Indonesian traditional herbal medicine towards rational phytopharmacological use. *Journal of Herbal Medicine, 4*(2), 51-73.

Wu, F., & Wang, T. (2013). Risk assessment of upper tract urothelial carcinoma related to aristolochic acid. *Cancer Epidemiology and Prevention Biomarkers*, cebp. 1386.2012.

Wu, J., LoRusso, P. M., Matherly, L. H., & Li, J. (2012). Implications of plasma protein binding for pharmacokinetics and pharmacodynamics of the γ-secretase inhibitor RO4929097. *Clinical Cancer Research, 18*(7), 2066-2079.

Wu, K., Jiang, L., Cao, J., Yang, G., Geng, C., & Zhong, L. (2007). Genotoxic effect and nitrative DNA damage in HepG2 cells exposed to aristolochic acid. *Mutation Research/Genetic Toxicology and Environmental Mutagenesis, 630*(1-2), 97-102.

Wu, X., Liu, J., Huang, H., Xue, W., Yao, X., & Jin, J. (2011). Interaction studies of aristolochic acid I with human serum albumin and the binding site of aristolochic acid I in subdomain IIA. *International journal of biological macromolecules, 49*(3), 343-350.

Yan, G. Z., Generaux, C. N., Yoon, M., Goldsmith, R. B., Tidwell, R. R., Hall, J. E., . . . Paine, M. F. (2012). A semiphysiologically based pharmacokinetic modeling approach to predict the dose-exposure relationship of an antiparasitic prodrug/active metabolite pair. *Drug metabolism and disposition, 40*(1), 6-17.

Yang, H., Zheng, X., Du, Y., Chen, Z., Zhu, D., & Lou, Y. (2011). Kinetics of aristolochic acid I after oral administration of Radix Aristolochiae or Guanxinsuhe preparation in canines. *J Ethnopharmacol, 135*(2), 569-574.

Yokoyama, Y., Sasaki, Y., Terasaki, N., Kawataki, T., Takekawa, K., Iwase, Y., . . . Ohta, S. (2018). Comparison of drug metabolism and its related hepatotoxic effects in HepaRG, cryopreserved human hepatocytes, and HepG2 cell cultures. *Biological and Pharmaceutical Bulletin*, b17-00913.

Yuan, J., Luo, X., Guo, M., Wu, J., Yang, W., Yu, R., & Yao, S. (2009). Determination of aristolochic acid I and its metabolites in cell culture with a hyphenated high-performance liquid chromatographic technique for cell toxicology. *Talanta, 78*(3), 1141-1147.

Zhang, L., Mu, X., Fu, J., & Zhou, Z. (2007). In vitro cytotoxicity assay with selected chemicals using human cells to predict target-organ toxicity of liver and kidney. *Toxicology in vitro, 21*(4), 734-740.

Zhang, M., van Ravenzwaay, B., Fabian, E., Rietjens, I. M., & Louisse, J. (2018). Towards a generic physiologically based kinetic model to predict in vivo uterotrophic responses in rats by reverse dosimetry of in vitro estrogenicity data. *Archives of toxicology, 92*(3), 1075-1088.

APPENDIX

APPENDIX I DATA MANAGEMENT TABLES

Table 10: Raw files

Name	Charlotte Koopmans
Registration number	930216464060
Start date of thesis	03-09-2018
Supervisor 1	Suparmi
Supervisor 2	Ivonne Rietjens
File path	**W:\PROJECTS\TOX_Research-data\Ivonne Rietjens\ Suparmi\2018_Charlotte Koopmans**

File name	Device	Description	Processed Y/N
UPLC analysis Empower\H-class\Charlotte Koopmans			
20181005_R_koopm079_1	UPLC H-class	Calibration curve 0-10 µM	N
20181005_R_koopm079_2	UPLC H-class	Calibration curve 20-100 µM	N
20181011_R_koopm079_1	UPLC H-class	Calibration curve 0-100 µM + jamu samples	N/Y
20181016_R_koopm079_1	UPLC H-class	Calibration curve 0-100 µM + jamu samples	N/Y
20181025_R_koopm079_01	UPLC H-class	Calibration curve 0-100 µM + jamu samples + spiked jamu samples (AA1, AA6, AA13, AA15)	N/Y/Y
20181114_R_koopm079_1	UPLC H-class	Calibration curve 0-25 µM + jamu samples + spiked jamu samples (AA1, AA10, AA11)	N/Y/Y
20182911_R_koopm079_1	UPLC H-class	Calibration curve 0-10 µM + spiked jamu samples (AA1, AA11)	Y
20181205_R_koopm079_1	UPLC H-class	Calibration curve 0-10 µM + spiked jamu samples (AA1, AA11)	Y
20190114_R_koopm079_1	UPLC H-class	Calibration curve 0-10 µM + spiked jamu samples (AA10)	Y
20190114_R_koopm079_2	UPLC H-class	Spiked jamu sample (AA10)	Y
Cytotoxicity assay (normal file path)			
20181114_R_koopm079_1	Spectrophotometer	WST-1 assay HepG2 cells 0-300 µM	Y
20181121_R_koopm079_1	Spectrophotometer	MTT assay HepG2 cells, not included in thesis 0-300 µM	N
20181128_R_koopm079_1	Spectrophotometer	WST-1 assay HepG2 cells 0-300 µM	Y

20181128_R_koopm079_2	Spectrophotometer	WST-1 assay HepG2 cells 0-300 µM	Y
20181205_R_koopm079_1	Spectrophotometer	WST-1 assay HepaRG cells 0-300 µM	Y
20181212_R_koopm079_1	Spectrophotometer	WST-1 assay HepaRG cells without FCS 0-300 µM	Y
20181213_R_koopm079_1	Spectrophotometer	WST-1 assay HepaRG cells without FCS 0-300 µM	Y
20190131_R_koopm079_1	Spectrophotometer	WST-1 assay HepG2 without FCS 0-300 µM	Y
LC-MS/MS analysis D:\from C\Rozaini\Charlotte			
20190122_1222019_01 tm 27	LC-MS/MS	Measurement DNA-adducts HepG2 cells 0-20 µM + Calibration curve 0-50 µM	Y
PBK modeling			
20190311_R_koopm079_5	Berkeley Madonna	PBK model code	Y
20190311_R_koopm079_51	Berkeley Madonna	PBK model outcome and comparison based on the amount of AA µM in the liver tissue	Y
20190311_R+P_koopm079_6	Berkeley Madonna	Sensitivity analysis of PBK model based on liver tissue + calculated normalized sensitivity coefficients.	Y

Table 11: Processed files

Name	Charlotte Koopmans
Registration number	930216464060
Start date of thesis	03-09-2018
Supervisor 1	Suparmi
Supervisor 2	Ivonne Rietjens
File path	**W:\PROJECTS\TOX_Research-data\Ivonne Rietjens\ Suparmi\2018_Charlotte Koopmans**

File name*	Program	Based on raw file(s)	Description	Presented in Figure
UPLC analysis				
20180925_R_koopm079_1	Excel	Jamu samples	Overview of all Indonesian jamu samples including ingredients from KNApSAcK Family.	Table 1
20181102_P_koopm079_01	Excel	20181011_R_koopm079_1 20181016_R_koopm079_1 20181025_R_koopm079_01 20181114_R_koopm079_1 20182911_R_koopm079_1 20181205_R_koopm079_1 20190114_R_koopm079_1 20190114_R_koopm079_2	Chromatograms of all samples, spiked samples, calibration curves. Calculations for LoD + LoQ, percentage of recovery, amount of aristolochic acids present in Indonesian jamu, EDI and MOE	Figure 4, 12 Table 2, 7, 8
Cytotoxicity assay				
20190204_R+P_koopm079_1	Excel	20181114_R_koopm079_1 20181121_R_koopm079_1 20181128_R_koopm079_1 20181128_R_koopm079_2 20181205_R_koopm079_1 20181212_R_koopm079_1 20181213_R_koopm079_1 20190131_R_koopm079_1	Processed data for concentration response-curves for cytotoxicity of HepaRG and HepG2 cells.	Figure 5 Table 3
20190311_P_koopm079_1	GraphPad Prism 5.0	20181114_R_koopm079_1 20181128_R_koopm079_1 20181128_R_koopm079_2 20190131_R_koopm079_1	Concentration-response curves cytotoxicity HepG2 cells incubated with and without FCS + IC_{10}	Figure 5 Table 3

20190311_P_koopm079_2	GraphPad Prism 5.0	20181205_R_koopm079_1 20181212_R_koopm079_1 20181213_R_koopm079_1	Concentration-response curves cytotoxicity HepaRG cells incubated with and without FCS + IC_{10}	Figure 5 Table 3
20190311_P_koopm079_7	GraphPad Prism 5.0		Dose response curves cytotoxicity HepG2 and HepaRG cells	Figure 9 Table 4
20190312_P_koopm079_1	Excel	PBK model	Calculation and correcting for the fraction unbound, reverse dosimetry by determining Odose mg, $BMDL_{10}$ calculations	Figure 9, 10 Table 4
LC-MS/MS analysis				
20190311_P_koopm079_3	GraphPad Prism 5.0	20190122_1222019_01 tm 27	Concentration-response curves DNA-adduct formation HepG2 cells incubated without FCS	Figure 6
20190204_P_koopm079_1	Excel	20190122_1222019_01 tm 27	Calculation of DNA-adducts per 10^8 nucleotides, nanodrop, translation to in vivo + $BMDL_{10}$ calculations	Figure 6, 10 Table 4
20190311_P_koopm079_71	GraphPad Prism 5.0	20190122_1222019_01 tm 27	Dose-response curves DNA-adducts in HepG2 cells	Figure 10
PBK modeling				
20190311_R_koopm079_52	GraphPad Prism 5.0	20190311_R_koopm079_51	PBK model outcome and comparison based on the amount of AA µM in the liver tissue	Figure 7
20190311_R+P_koopm079_61	Excel	20190311_R_koopm079_5	Normalized sensitivity coefficients	Figure 8
Risk assessment				
20190322_koopm079_1	GraphPad Prism 5.0	20181011_R_koopm079_1 20181016_R_koopm079_1 20181025_R_koopm079_01 20181114_R_koopm079_1 20182911_R_koopm079_1 20181205_R_koopm079_1 20190114_R_koopm079_1 20190114_R_koopm079_2	MOE values for the risk assessment of kidney and liver cytotoxicity.	Figure 11